Neuron

Article

Absence of familiarity triggers hallmarks of autism in mouse model through aberrant tail-of-striatum and prelimbic cortex signaling

Graphical abstract

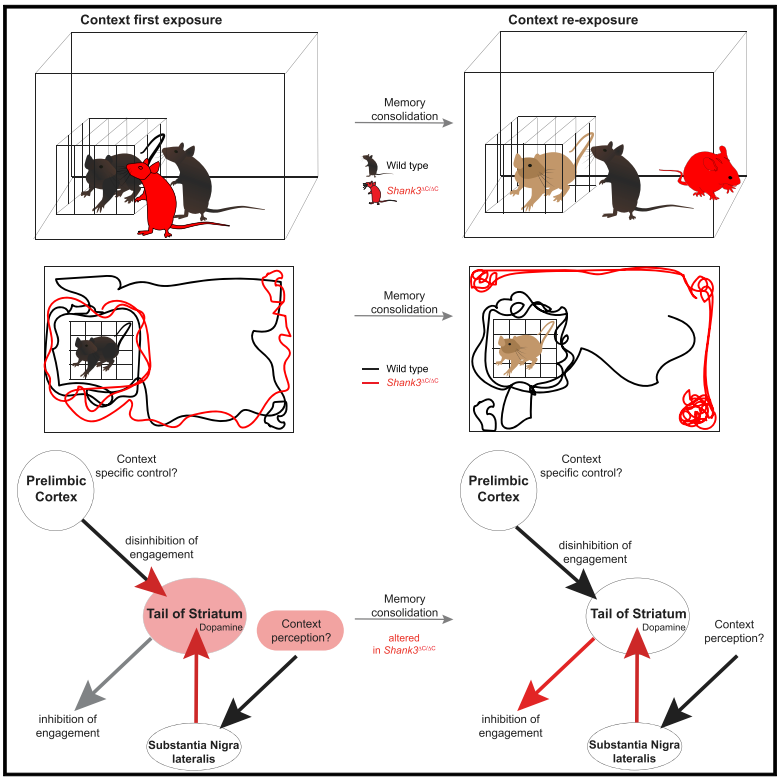

Highlights

- Novel context exposure induces autism behavior upon re-exposure in *Shank3*$^{\Delta C/\Delta C}$ mice
- Elevated TS DA release in novel context in *Shank3*$^{\Delta C/\Delta C}$ mice
- PreL to TS connectivity ensures engagement at re-exposure in wild type
- Inclusion of familiar features rescues DA release and engagement in *Shank3*$^{\Delta C/\Delta C}$

Authors

Sebastian Krüttner, Antonio Falasconi, Sergio Valbuena, Ivan Galimberti, Tewis Bouwmeester, Silvia Arber, Pico Caroni

Correspondence

caroni@fmi.ch

In brief

Aversion toward unfamiliarity is a hallmark of autism. Kruettner et al. show that in *Shank3*$^{\Delta C/\Delta C}$ autism model mice, exposure to novel environments lacking familiar features produces failure to engage and repetitive behaviors upon context re-exposure. Therefore, behavioral therapies involving familiarity might prevent the emergence of autism phenotypes in predisposed individuals.

Krüttner et al., 2022, Neuron *110*, 1468–1482
May 4, 2022
https://doi.org/10.1016/j.neuron.2022.02.001

CellPress

CellPress
OPEN ACCESS

Neuron

Article

Absence of familiarity triggers hallmarks of autism in mouse model through aberrant tail-of-striatum and prelimbic cortex signaling

Sebastian Krüttner,[1,5] Antonio Falasconi,[1,2] Sergio Valbuena,[1] Ivan Galimberti,[3] Tewis Bouwmeester,[4] Silvia Arber,[1,2] and Pico Caroni[1,6,*]

[1]Friedrich Miescher Institute, Basel, Switzerland
[2]Biozentrum University of Basel, Basel, Switzerland
[3]Department of Neuroscience, Novartis Inst. for Biomed. Res., Basel, Switzerland
[4]Chemical Biology and Therapeutics, Novartis Inst. for Biomed. Res., Basel, Switzerland
[5]Present address: Harvard Medical School, Department of Neurobiology, Boston, MA, USA
[6]Lead contact
*Correspondence: caroni@fmi.ch
https://doi.org/10.1016/j.neuron.2022.02.001

SUMMARY

Autism spectrum disorder (ASD) involves genetic and environmental components. The underlying circuit mechanisms are unclear, but behaviorally, aversion toward unfamiliarity, a hallmark of autism, might be involved. Here, we show that in *Shank3*$^{\Delta C/\Delta C}$ ASD model mice, exposure to novel environments lacking familiar features produces long-lasting failure to engage and repetitive behaviors upon re-exposure. Inclusion of familiar features at first context exposure prevented enhanced dopamine transients in tail of striatum (TS) and restored context-specific control of engagement to wild-type levels in *Shank3*$^{\Delta C/\Delta C}$ mice. Engagement upon context re-exposure depended on the activity in prelimbic cortex (PreL)-to-TS projection neurons in wild-type mice and was restored in *Shank3*$^{\Delta C/\Delta C}$ mice by the chemogenetic activation of PreL→TS projection neurons. Environmental enrichment prevented ASD-like phenotypes by obviating the dependence on PreL→TS activity. Therefore, novel context experience has a key role in triggering ASD-like phenotypes in genetically predisposed mice, and behavioral therapies involving familiarity and enrichment might prevent the emergence of ASD phenotypes.

INTRODUCTION

Autism spectrum disorder (ASD) is a neurodevelopmental disease associated with a core of behavioral abnormalities, including social deficits, verbal and intellectual disabilities, insistence on sameness, sensory abnormalities and increased stereotypic behavioral patterns (Baron-Cohen and Belmonte, 2005; Bourgeron, 2015; Chen et al., 2015; Geschwind, 2009; Jiujias et al., 2017). Whether and to what extent genetically predisposed individuals develop ASD is influenced by environmental components (Baron-Cohen and Belmonte, 2005; Bourgeron, 2015; Chen et al., 2015), and relatives with closely comparable genetic backgrounds can differ greatly in the extent to which they develop ASD symptoms (Bailey et al., 1998; Pisula and Ziegart-Sadowska, 2015; Ronald and Hoekstra, 2011). Which elements of experience might influence the emergence of ASD is not clear (Baum et al., 2015; Robertson and Baron-Cohen, 2017). However, given the mostly complex multigenic basis of ASD predisposition, the identification of environmental factors affecting individuals from a range of predisposed genetic backgrounds would have important therapeutic implications (Baron-Cohen and Belmonte, 2005; Bourgeron, 2015; Chen et al., 2020; Geschwind, 2009; Jamal et al., 2021; Sahin and Sur, 2015).

It is currently unclear whether different ASD-linked phenotypes arise and develop independently or whether there might be singular causes that influence a range of behavioral abnormalities in ASD (Chen et al., 2020; Geschwind, 2009; Sahin and Sur, 2015). The identification of causal relationships among core behavioral phenotypes in ASD would provide useful indications as to relevant environmental factors and underlying brain circuit mechanisms (Baron-Cohen and Belmonte, 2005; Bourgeron, 2015; Sahin and Sur, 2015).

Alterations in sensory perception and aversion toward uncertainty are core features of ASD (Baum et al., 2015; Bourgeron, 2015; Chen et al., 2020; Jiujias et al., 2017; Leekam et al., 2007; Orefice et al., 2016; Robertson and Baron-Cohen, 2017; Rodriguez and Thompson, 2015). How these might relate to the observed characteristic engagement deficits has remained unclear (Rodriguez and Thompson, 2015). Mechanistically, engagement is thought to involve prefrontal-striatal circuits

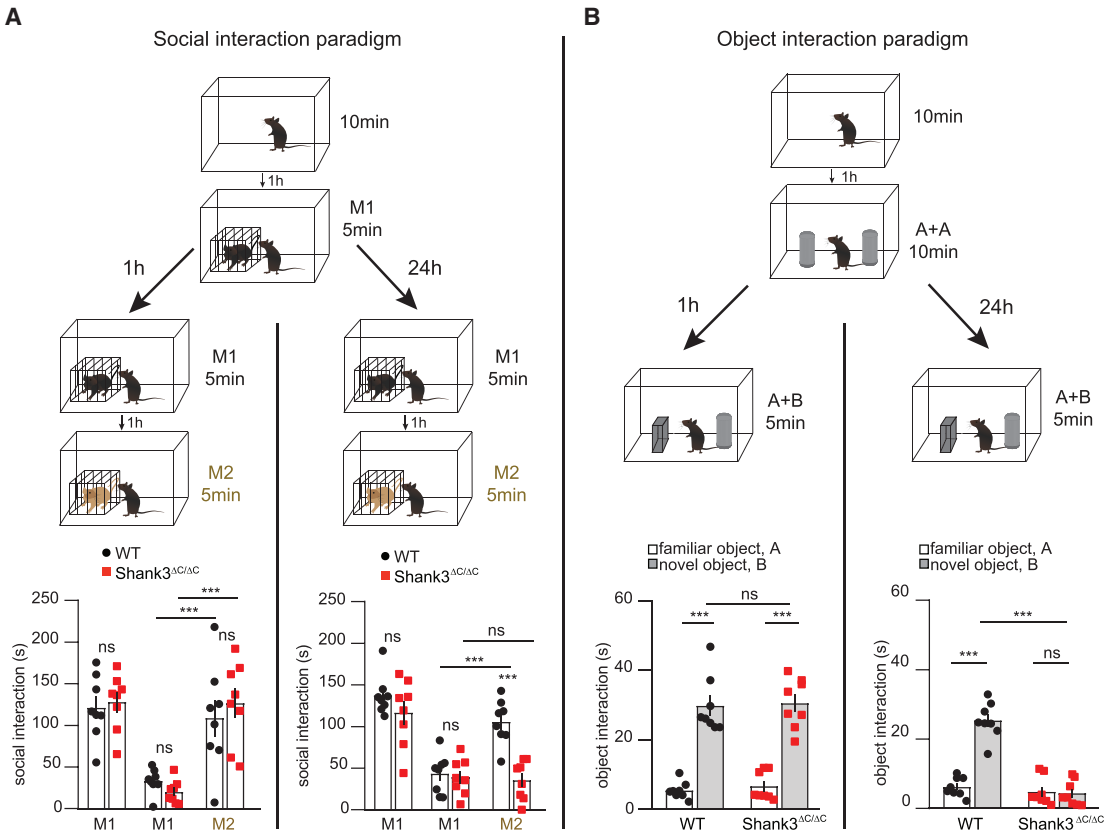

Figure 1. Delayed failure to explore novel conspecifics or objects in *Shank3*$^{\Delta C/\Delta C}$ mice

(A) Social interaction. Top: schematic of social interaction paradigm. Novel context: large empty box with tester animal.

(B) Object interaction. Top: schematic of object exploration paradigm.

For all panels: n = 8; values are means ± SEM; two-way-RM-ANOVA, Sidak's post hoc test; ns = non significant, $p < 0.001$ (**), $p < 0.0001$ (***); black circles (WT) and red squares (*Shank3*$^{\Delta C/\Delta C}$) indicate values from individual mice.

and modulation of striatal circuitry by dopamine (DA) (Balleine and O'Doherty, 2010; Gerfen and Surmeier, 2011; Woon et al., 2020). Furthermore, novel context experience facilitates new learning through recruitment of prelimbic cortex (PreL) through ventral hippocampus (Park et al., 2021). Among dorsal striatal areas, the tail of striatum (TS) mediates avoidance behavior toward objects, which is enhanced through DA release by substantia nigra reticulata lateralis neuron projections to TS (Jiang and Kim, 2018; Menegas et al., 2018; Menegas et al., 2015). Accordingly, a hypothetical scenario of how novelty might influence engagement in ASD could be through context-related DA release in TS and prefrontal control of TS neurons.

Most ASD patients represent idiopathic cases, but among those with a known genetic origin, 1% of patients diagnosed with ASD are those with Phelan-McDermid syndrome, which exhibit loss of *Shank3* due to rearrangements of chromosome 22q13 (Durand et al., 2007; Phelan and McDermid, 2012). Furthermore, *de novo* mutations in *Shank3* are associated with nonsyndromic ASD and intellectual disability (Gauthier et al., 2009; Moessner et al., 2007). Importantly, several studies identified aversion toward novelty as a key feature of *Shank3* mutant animals (Drapeau et al., 2018; Jaramillo et al., 2016; Kouser et al., 2013; Speed et al., 2015). However, how *Shank3*-related alterations in neocortex, striatum, and ventral hippocampus (see STAR Methods) might trigger ASD-like phenotypes has remained unclear.

Here, we investigated whether and how context-related engagement might be affected in genetically predisposed *Shank3*$^{\Delta C/\Delta C}$ ASD model mice (Bidinosti et al., 2016) and whether that might account for the manifestation of ASD-like phenotypes. Our results reveal that experience of novel context in the absence of familiar features causes ASD-linked phenotypes in *Shank3*$^{\Delta C/\Delta C}$ mice upon context re-exposure. Together, our findings suggest that therapies based on familiarity and enrichment may have a major impact on autistic symptoms in predisposed individuals.

RESULTS

Delayed failure to explore novel conspecifics or objects in *Shank3*$^{\Delta C/\Delta C}$ mice

To investigate a possible relationship between experiencing a context and the degree of engagement in ASD, we first compared WT and *Shank3*$^{\Delta C/\Delta C}$ (Bidinosti et al., 2016; see STAR Methods) mice in context-related social and object interaction tasks. In this study, we use the term "context" to refer

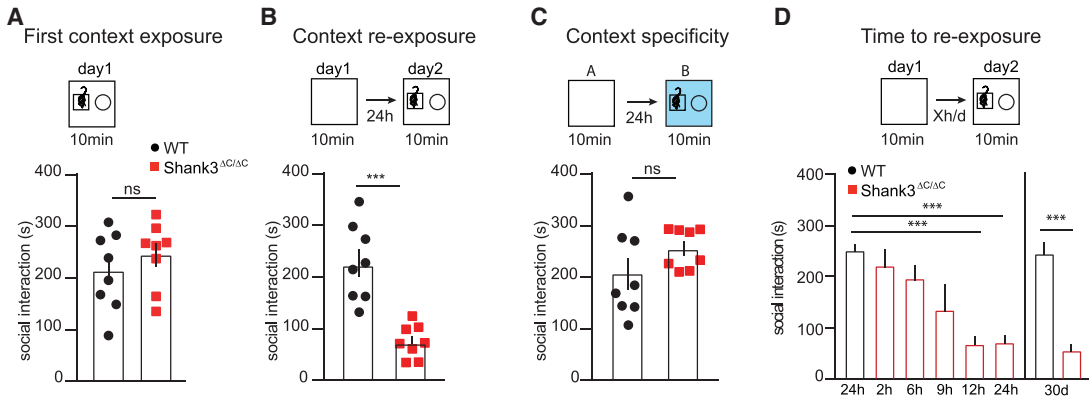

Figure 2. Experience-dependent context-specific failure to engage in *Shank3*$^{\Delta C/\Delta C}$ mice

(A and B) Specific relationship between reduced social interaction and context re-exposure in mutant mice. In *Shank3*$^{\Delta C/\Delta C}$ mice, social interaction is indistinguishable from WT at initial context exposure (day 1, A) but greatly impaired at context re-exposure on the next day (day 2, B).

(C and D) Failure to interact with conspecific is context specific (not detected in novel context B) (C) and long lasting (D). Robust reduction in social exploration is detected in *Shank3*$^{\Delta C/\Delta C}$ animals from 12 h upon first exposure to novel context and lasts for at least 30 days (D).

For all panels: n = 8; values are means ± SEM; unpaired Student t tests, Tukey's post hoc test (A–C); two-way-RM-ANOVA, Sidak's post hoc test (D); ns = non significant, $p < 0.0001$ (***); black circles (WT) and red squares (*Shank3*$^{\Delta C/\Delta C}$) indicate values from individual mice.

to all aspects of an experimental environment (e.g., boundaries, textures, colors, and odors), except objects (e.g., falcon tubes) or conspecifics with which mice can engage. Young adult (8–9 weeks) male mice were introduced to a novel context for 10 min and tested for social or object interactions and memory recall upon reintroduction to that same context (Figures 1A and 1B). Upon reintroduction into the same context and in 1 h short-term recall tests, *Shank3*$^{\Delta C/\Delta C}$ mice exhibited social investigation toward novel or familiar intruder mice indistinguishable from WT mice (novel: WT 121.2 ± 13.5 s, *Shank3*$^{\Delta C/\Delta C}$ 128.1 ± 11.9 s, p = 0.9801; short-term recall familiar: WT 33.2 ± 5.3 s, *Shank3*$^{\Delta C/\Delta C}$ 20.2 ± 4.9 s, p = 0.8859; short-term recall novel: WT 108.9 ± 5.3 s, *Shank3*$^{\Delta C/\Delta C}$ 126.9 ± 4.9 s, p = 0.7488; Figure 1A, left). Much in contrast, *Shank3*$^{\Delta C/\Delta C}$ mice failed to exhibit increased exploration toward novel intruder mice when tested 24 h after first exposure (novel intruder: WT 105.6 ± 9.4 s, *Shank3* *Shank3*$^{\Delta C/\Delta C}$ 35.7 ± 8.2 s, $p < 0.0001$; Figure 1A, right). WT and *Shank3*$^{\Delta C/\Delta C}$ mice also exhibited equal levels of enhanced exploration toward an introduced novel object when tested 1 h after initial exposure to novel context (novel object: WT 29.74 ± 2.9 s, *Shank3*$^{\Delta C/\Delta C}$ 30.51 ± 2.5 s, p = 0.9600; Figure 1B, left), but mutant mice failed to exhibit enhanced exploration of novel objects in 24 h recall experiments (novel object: WT 25.4 ± 1.8 s, *Shank3*$^{\Delta C/\Delta C}$ 4.4 ± 1.3 s, $p < 0.0001$; Figure 1B, right). Thus, rather than engagement deficits per se, *Shank3*$^{\Delta C/\Delta C}$ mice exhibit failure to explore novel conspecifics or objects at long-term recall, but not within 1 h of first context exposure. This might reflect a deficit to engage upon long-term recall or a deficit to detect the new conspecific or object as novel at long-term recall.

Experience-dependent context-specific failure to engage in *Shank3*$^{\Delta C/\Delta C}$ mice

23We next investigated the possibility that exposure of *Shank3*$^{\Delta C/\Delta C}$ mice to a new context per se might lead to subsequently reduced exploration of conspecifics and objects in that context. Applying no context pre-exposure, we found that WT and *Shank3*$^{\Delta C/\Delta C}$ mice exhibited an indistinguishable level of engagement within a novel context in which conspecifics are present (social: WT 212.9 ± 26.8 s, *Shank3*$^{\Delta C/\Delta C}$ 244.6 ± 22.6 s, p = 0.3823; Figure 2A). By contrast, pre-exposure to a novel context (here indicated as an empty rectangular box) without any additional cue (e.g., objects or conspecifics) induced a drastic decrease in social interactions within the same context on the next day in *Shank3*$^{\Delta C/\Delta C}$ but not WT mice (social: WT 227.3 ± 26.3 s, *Shank3*$^{\Delta C/\Delta C}$ 74.82 ± 11.4 s, $p < 0.0001$; Figure 2B). This failure to interact upon context re-exposure in *Shank3*$^{\Delta C/\Delta C}$ mice was specific to the previously experienced context (A) since no interaction deficits were detected when mutant mice were tested in a different (i.e., novel) context (B) on the next day (Figure 2C). Context-specific failure to engage in *Shank3*$^{\Delta C/\Delta C}$ mice was a long-lasting phenomenon, which was detected from about 12 h after initial exposure to novel context and with undiminished strength up to at least 1 month after initial exposure (Figure 2D). Taken together, these findings provide evidence that *Shank3*$^{\Delta C/\Delta C}$ mice exhibit long-lasting, context-specific failure to engage toward conspecifics or objects, starting from about 12 h after initial exposure to novel context.

Context-specific failure to engage triggers ASD-like phenotypes in *Shank3*$^{\Delta C/\Delta C}$ mice

To determine the precise nature of context-specific behavioral abnormalities that *Shank3*$^{\Delta C/\Delta C}$ mice might exhibit, we closely monitored their behavior upon initial context exposure and re-exposure. Monitored behavioral patterns included aspects commonly reported in ASD studies, such as interaction with objects and social cues as indicated by rearing and sniffing (% exploration), self-centered behaviors involving stereotypic forth backward and sideward moving as well as self-grooming (% self-centered behavior) and total distance translocated (Ferhat et al., 2017; Pasciuto et al., 2015; Schroeder et al., 2017). Spontaneous explorative and self-centered behaviors were indistinguishable between WT and *Shank3*$^{\Delta C/\Delta C}$ mice at first exposure

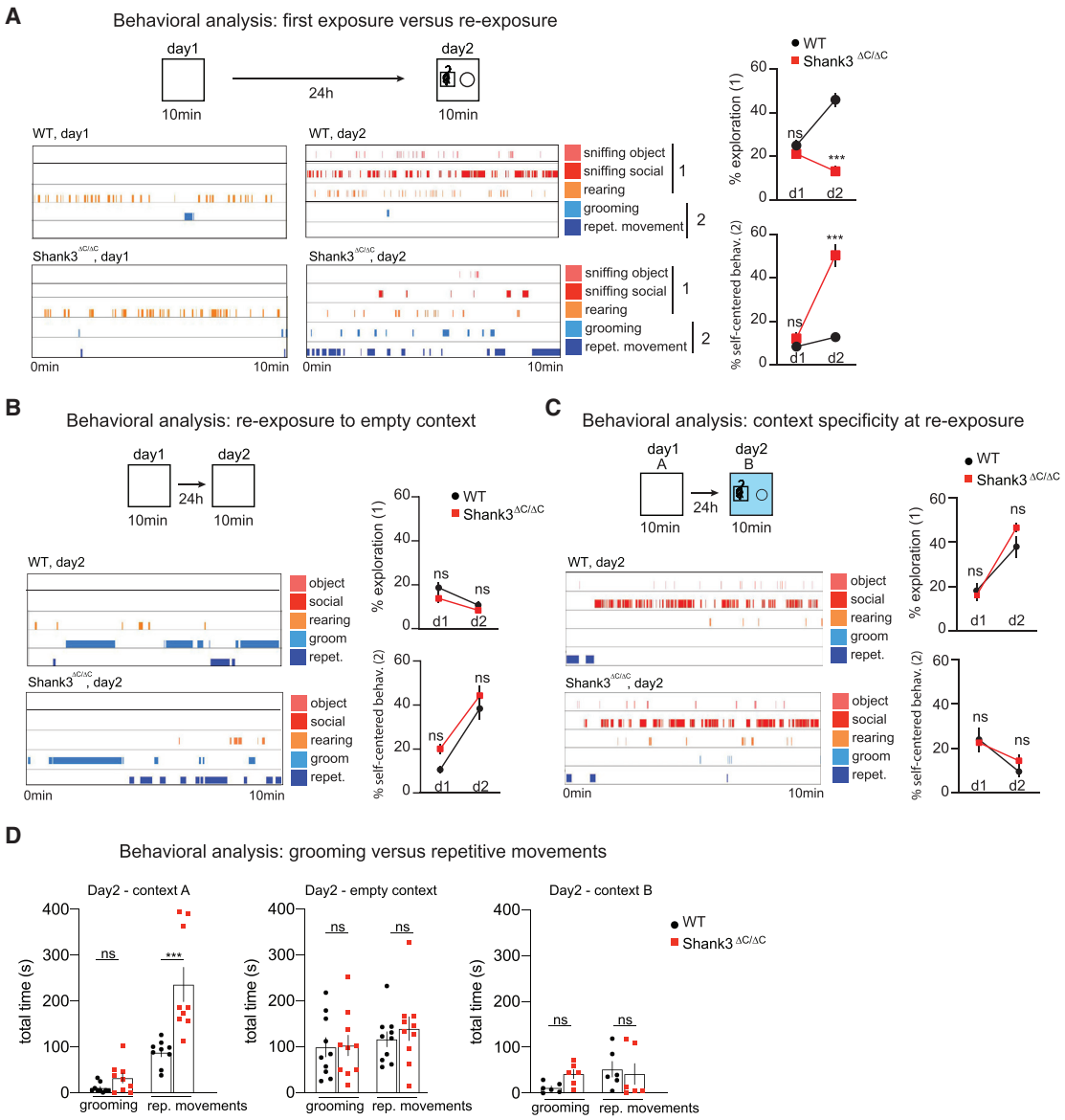

Figure 3. Context-specific failure to engage triggers ASD-like phenotypes in *Shank3*$^{\Delta C/\Delta C}$ mice

(A–D) Behavioral analysis during first exposure to novel context and at re-exposure in the presence of con-specific and object (A), at re-exposure in the absence of con-specific or object (B), and at exposure to a different novel context on day2 (C). Bin plots of behavior versus time for representative WT and *Shank3*$^{\Delta C/\Delta C}$ mice (left), and quantitative analysis of explorative behaviors (1; engagement and rearing) and self-centered behaviors (2) (right; grooing and repetitive movements). Analysis of self-centered behaviors (grooming, repetitive movements) under conditions as in (A–C) (D).

Grouped data and statistical analysis for exploratory and self-centered behaviors on day 1 and day 2. For all panels: n = 8; values are means ± SEM; two-way-RM-ANOVA, Sidak's post hoc test; ns = non significant, p < 0.0001 (***); black circles (WT) and red squares (*Shank3*$^{\Delta C/\Delta C}$) indicate grouped values.

to novel context (initial exposure on day 1; Figure 3A). By contrast, context re-exposure after 24 h was consistently associated with protracted bouts of self-centered behaviors and with reduced exploration time in *Shank3*$^{\Delta C/\Delta C}$ mice (day 2; Figure 3A). Context re-exposure in the absence of objects or conspecifics resulted in indistinguishable reduced exploratory behavior and enhanced self-centered behaviors in WT and *Shank3*$^{\Delta C/\Delta C}$ mice (Figure 3B), but these behaviors were not overrepresented in a different novel context B (Figure 3C). Quantitative analysis of grooming and repetitive movement behaviors confirmed that these were specifically enhanced upon context re-exposure in WT and *Shank3*$^{\Delta C/\Delta C}$ mice (Figure 3D). Notably, however, *Shank3*$^{\Delta C/\Delta C}$ mice specifically exhibited elevated levels of repetitive movements compared with WT mice upon context re-exposure in the presence of items to potentially engage with (here a conspecific and an object), whereas in the absence of such items, grooming behavior was enhanced in both genotypes upon context re-exposure, and no differences in repetitive

movements were detected between WT and *Shank3*$^{\Delta C/\Delta C}$ mice (Figure 3D). Total distance translocated was indistinguishable between WT and *Shank3*$^{\Delta C/\Delta C}$ mice throughout all experimental conditions (Figure S1). These findings suggest that in *Shank3*$^{\Delta C/\Delta C}$ mice enhanced levels of repetitive movements reminiscent of core hallmarks of ASD (Jiujias et al., 2017; Pasciuto et al., 2015) are specifically associated with failure to engage upon re-exposure to novel context after more than 12 h.

To explore a possible relationship between anxiety and failure to engage in *Shank3*$^{\Delta C/\Delta C}$ mice, we tested WT and *Shank3*$^{\Delta C/\Delta C}$ mice for anxiety-related behavior on two consecutive days in an elevated plus maze. On the first day, *Shank3*$^{\Delta C/\Delta C}$ mice spent more time in open arms compared with WT littermates, arguing against the possibility that they might be generally more anxious (Figure S1). By contrast and consistent with the notion that re-exposure to a novel context induces anxiety-like behavior in *Shank3*$^{\Delta C/\Delta C}$ mice, mutant mice exhibited greatly enhanced open arms avoidance on the second day of elevated plus maze exposure (Figure S1).

DA release and memory induced in TS at first exposure to novel context account for failure to engage upon re-exposure in *Shank3*$^{\Delta C/\Delta C}$ mice

We next aimed to elucidate the circuit mechanisms underlying context-specific failure to engage and the possible prevention thereof in *Shank3*$^{\Delta C/\Delta C}$ mice. To determine whether context-specific engagement might involve the TS, we carried out chemical lesions of dopaminergic axon terminals specifically in TS with local application of 6-hydroxydopamine (6-OHDA, Figures 4A and S2). The chemical lesions of dopaminergic axon terminals in TS 24 h before initial exposure to a novel context abolished failure to engage with conspecifics at context re-exposure in *Shank3*$^{\Delta C/\Delta C}$ mice (WT 235.4 ± 14.1 s, *Shank3*$^{\Delta C/\Delta C}$ 221.2 ± 37.9 s, $p = 0.9046$; Figure 4A, middle panel). Moreover, a robust increase in engagement upon context re-exposure could be observed in WT and *Shank3*$^{\Delta C/\Delta C}$ mice when assessing interactions with objects, with *Shank3*$^{\Delta C/\Delta C}$ mice now exhibiting strong preferential exploration of novel objects (WT 67.97 ± 11.9 s, *Shank3*$^{\Delta C/\Delta C}$ 36.77 ± 4.4 s, $p < 0.0001$; Figure 4A, right panel). These findings pointed to TS as a striatal area involved in context-specific control of engagement in WT and *Shank3*$^{\Delta C/\Delta C}$ mice.

We next sought to determine whether DA release in TS upon first exposure (day 1) differed between WT and *Shank3*$^{\Delta C/\Delta C}$ mice. We recorded TS DA as mice repeatedly approached and retreated from a novel object with the specific fluorescent sensor dLight1.3b (Patriarchi et al., 2018) expressed in TS neurons (Figure S2). Mice were exposed to a novel context for 5 min, and then immediately let to interact with an introduced novel object for additional 10 min. Strikingly, approach-and retreat-related DA transients in TS were greatly elevated in *Shank3*$^{\Delta C/\Delta C}$ mice compared with WT mice (Figure 4B, left). Furthermore, while DA transients in TS habituated upon repeated approaches of the object in WT mice, they exhibited pronounced approach-related variability in *Shank3*$^{\Delta C/\Delta C}$ mice (Figure 4B).

We next investigated the possibility that a memory induced in TS upon first exposure to novel context might lead to reduced engagement upon re-exposure in *Shank3*$^{\Delta C/\Delta C}$ mice. Local D1/5 DA receptor (D1/5R) signaling in task-related areas during a time window 12–15 h after acquisition is critically important for long-term memory consolidation in a variety of learning settings and their associated brain areas (Rossato et al., 2009; Katche et al., 2013; Krüttner et al., 2015; Karunakaran et al., 2016). This prompted us to carry out experiments in which we locally treated mice in TS with D1/5R antagonist 12 h after initial context exposure and tested the impact of these interventions on engagement upon context re-exposure. Indeed, when WT or *Shank3*$^{\Delta C/\Delta C}$ mice were treated locally in TS with D1/5R antagonist 12 h after first context exposure, engagement upon re-exposure closely mimicked values detected upon ablation of dopaminergic axons in TS (Figure 4C).

Taken together, these results are consistent with the notion that a memory induced in TS upon elevated DA transients during first exposure accounts for reduced engagement at re-exposure in *Shank3*$^{\Delta C/\Delta C}$ mice.

Engagement at context re-exposure depends on activity in PreL→TS projection neurons

To understand how WT mice still engage upon context re-exposure in spite of approach-related TS DA transients at first exposure, we hypothesized that TS-related avoidance induced upon first exposure might be counteracted by inputs from other brain areas. To identify inputs to TS that might additionally control engagement, we carried out retrograde tracing experiments from TS (see Figure S3 and STAR Methods for details). In addition to sensory and premotor areas, brain areas projecting to TS included medial prefrontal cortex areas that have been implicated in ASD such as PreL and anterior cingulate cortex (ACC; a prefrontal area adjacent to PreL), as well as basolateral amygdala (BLA); (Brumback et al., 2018; Guo et al., 2019; Valjent and Gangarossa, 2021) (Figure S3). Based on these findings, we determined whether silencing ASD-linked prefrontal areas containing projection neurons to TS might influence engagement upon context re-exposure in WT mice. Silencing PreL, a prefrontal area that has been related to social engagement (Levy et al., 2019), through chemogenetic activation of PreL PV neurons in *PV-Cre* mice (Magnus et al., 2011; Figure S3) during context re-exposure specifically led to failure to engage with conspecifics (Figure 5A) or objects (Figure 3) in *PV-Cre* mice. Strikingly, these now exhibited lack of engagement indistinguishable from *Shank3*$^{\Delta C/\Delta C}$ mice. In contrast, the same PreL treatment did not further reduce engagement toward conspecifics in *PV-Cre*;*Shank3*$^{\Delta C/\Delta C}$ mice (Figure 5A). PV neuron-mediated silencing of other areas projecting to TS, including ACC, or BLA did not noticeably affect context-specific engagement in *PV-Cre* mice (Figures 5A and S3).

Consistent with the notion that the inputs from PreL to TS are important for engagement, chemogenetic silencing of retrogradely targeted PreL→TS projection neurons with an inhibitory PSAM construct effectively prevented engagement toward intruders (Figure 5B) and objects (Figure S3) at context re-exposure in WT mice (PreL→TS intruder: WT Saline 256.4 ± 19.1 s, WT PreL→TS silencing 101.1 ± 22.4 s, $p < 0.0001$; *Shank3*$^{\Delta C/\Delta C}$ PreL→TS silencing 62.0 ± 29.9 s, $p = 0.3757$; Figure 5B). Furthermore, consistent with the notion that PreL acts through PreL→TS projection neurons to control engagement, we did not detect obvious differences between the impact of PreL or PreL→TS projection neuron silencing at re-exposure in WT and *Shank3*$^{\Delta C/\Delta C}$ mice

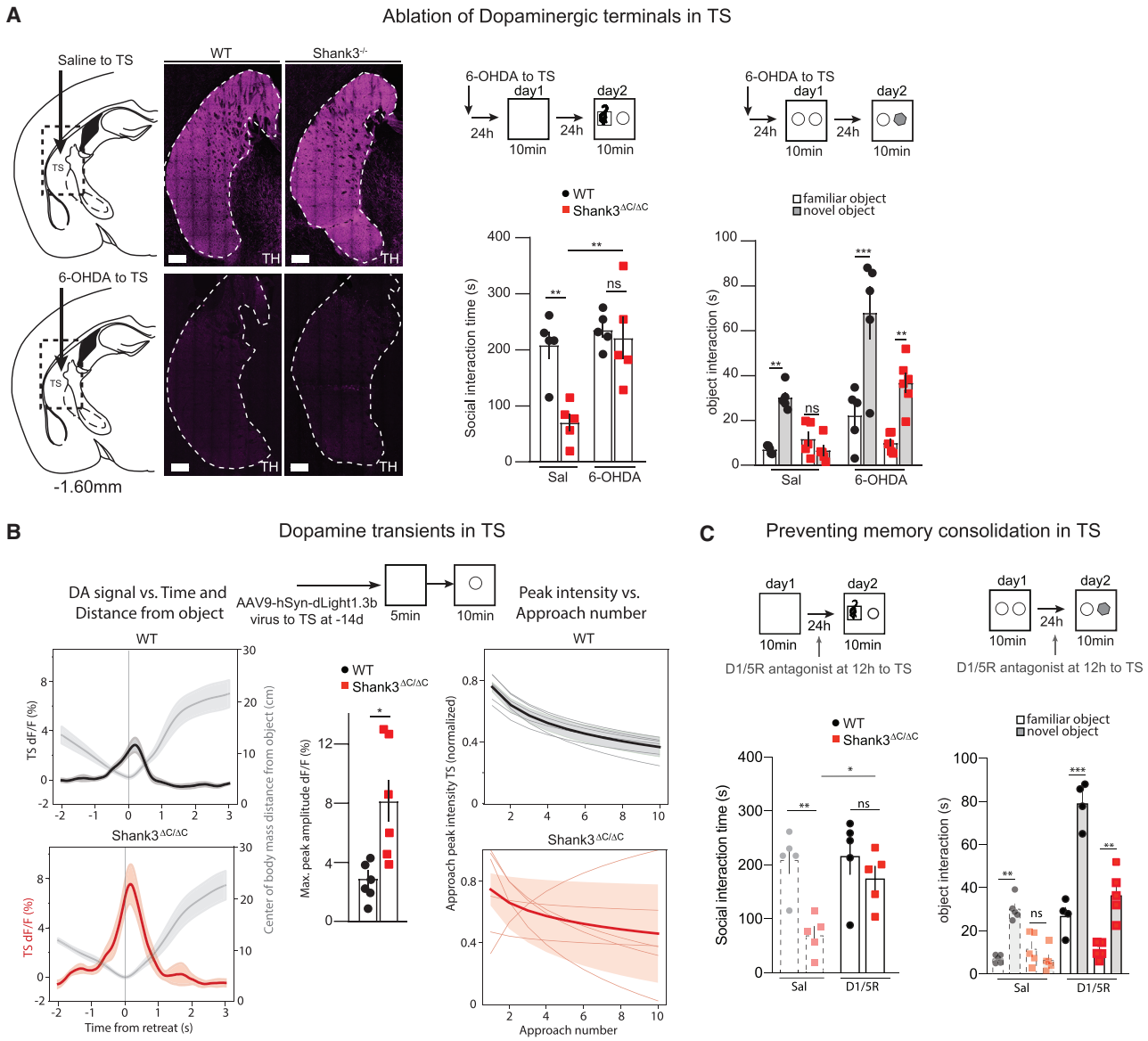

Figure 4. DA release and memory induced in TS at first exposure to novel context account for failure to engage upon re-exposure in *Shank3*$^{\Delta C/\Delta C}$ mice

(A) Left: representative images of TS illustrating loss of tyrosine hydroxylase (TH) labeling following ablation of dopaminergic axon terminals by local injection of 6-hydroxydopamine (6-OHDA). Right: Ablation of dopaminergic axon terminals in TS rescues engagement with conspecifics (left panel) and increases interactions with novel objects (right panel) upon novel context re-exposure in *Shank3*$^{\Delta C/\Delta C}$ mice.

(B) Enhanced retreat-related DA transients in TS at novel context exposure in *Shank3*$^{\Delta C/\Delta C}$ mice.

(C) Preventing memory consolidation in TS mimicks effects of DA axon ablation in TS on social (left) and object (right) engagement in WT and *Shank3*$^{\Delta C/\Delta C}$ mice. Dashed bars: values upon DA axon ablation are replotted (from A, saline) for comparison.

For all panels: n ≥ 5; values are means ± SEM; two-way-RM-ANOVA, Sidak's post hoc test; ns = non significant $p < 0.05$ (*), $p < 0.001$ (**) $p < 0.0001$ (***); black circles (WT) and red squares (*Shank3*$^{\Delta C/\Delta C}$) indicate values from individual mice. Scale bars, 200 μm.

(Figures 5A, 5B, and S3). In control experiments involving PreL→TS mock silencing with a virus lacking the chemogenetic silencing PSAM construct, no effects on engagement were detected in WT mice (Figure S3). To determine whether PreL→TS neurons also project to other brain regions through which these behavioral phenotypes could be mediated, we combined retrograde tracing from TS with anterograde tracing from PreL (AAV-DIO-Synaptophysin-eGFP, Figure S3). We found that PreL→TS neurons collateralized to BLA (Figure S4). However, supporting the notion that it was specifically the inputs from PreL to TS that were important for engagement, PSAM-mediated silencing of BLA→TS or ACC→TS projection neurons did not affect engagement in WT mice (Figure S4). Taken together, these results provided evidence that in WT mice, exposure to a novel context is followed by context-specific

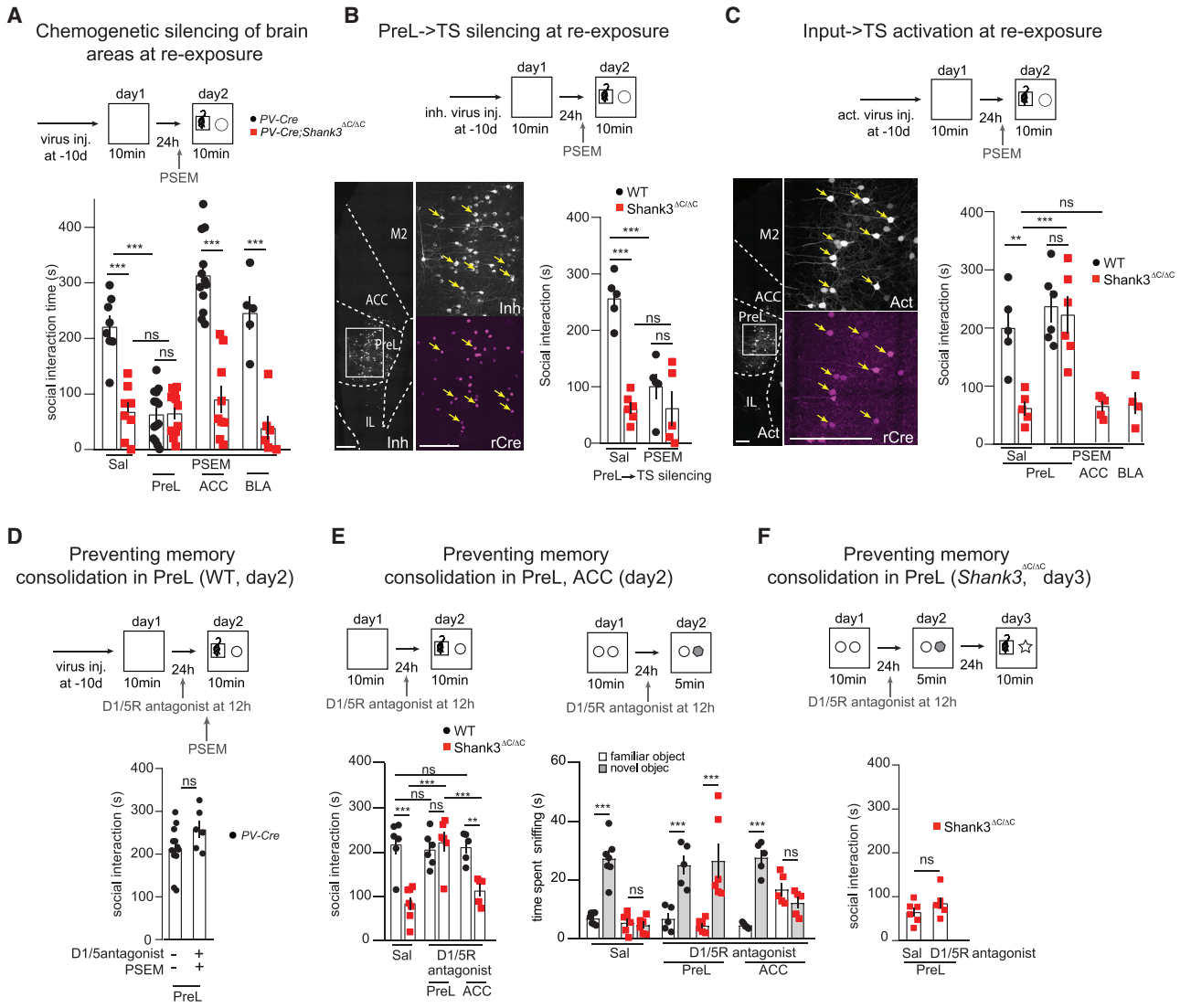

Figure 5. Engagement at context re-exposure depends on activity in PreL→TS projection neurons

(A and B) Silencing of PreL (A; but not ACC or BLA) or of PreL→TS projection neurons (B) during context re-exposure suppresses social exploration in WT mice.

(C) Activation of PreL→TS, but not ACC→TS or BLA→TS projection neurons during context re-exposure rescues social exploration in *Shank3*$^{\Delta C/\Delta C}$ mice.

(D) Preventing memory consolidation in WT PreL abrogates PreL requirement to promote social engagement at context re-exposure (day 2 becomes day 1).

(E) Interference with memory consolidation in PreL (but not ACC) rescues social (left) and novel object (right) engagement upon context re-exposure in *Shank3*$^{\Delta C/\Delta C}$.

(F) Social exploration in *Shank3*$^{\Delta C/\Delta C}$ upon context re-exposure on day 3 does not benefit from interference with memory consolidation 12 h after first context exposure (day 3 becomes day 2).

For all panels: n ≥ 5; values are means ± SEM; unpaired Student t tests, Tukey's post hoc test (D and F), or two-way-RM-ANOVA, Sidak's post hoc test (A–C and E); ns = non significant p < 0.01 (**), p < 0.0001 (***); black circles (WT) and red squares (*Shank3*$^{\Delta C/\Delta C}$) indicate values from individual mice. Scale bars, 200 μm.

engagement toward conspecifics or objects specifically mediated by activity in PreL→TS projection neurons.

Chemogenetic activation of PreL→TS projection neurons at context re-exposure sufficient to prevent lack of engagement in *Shank3*$^{\Delta C/\Delta C}$ mice

To determine whether artificially activating PreL→TS projection neurons at context re-exposure might be sufficient to promote engagement upon context re-exposure in *Shank3*$^{\Delta C/\Delta C}$ mice, we carried out corresponding chemogenetic activation experiments delivering an activator PSAM construct to PreL→TS projection neurons. Indeed, chemogenetic activation of PreL→TS projection neurons at context re-exposure in *Shank3*$^{\Delta C/\Delta C}$ mice was sufficient to restore engagement toward conspecifics to levels indistinguishable from those exhibited by WT mice (intruder: WT PreL→TS act. 237.7 ± 27.4 s, *Shank3*$^{\Delta C/\Delta C}$ PreL→TS act. 223.1 ± 31.5, p = 0.9065; *Shank3*$^{\Delta C/\Delta C}$ Saline 62.4 ± 12.0 s, p = 0.0009; Figure 5C). In experiments controlling

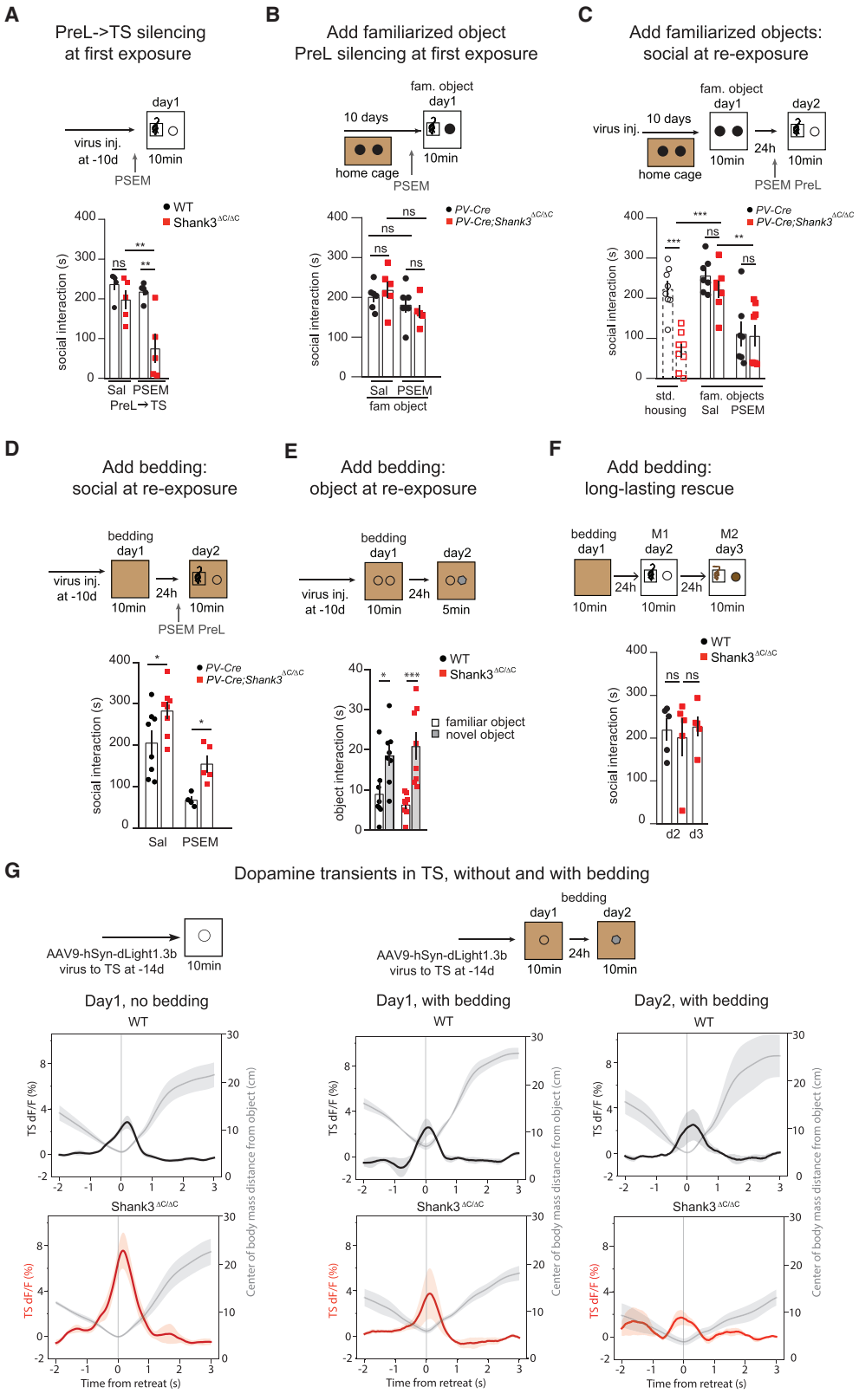

(legend on next page)

for specificity of the PreL→TS mechanism, activation of ACC→TS or BLA→TS connectivity did not improve engagement in *Shank3*$^{\Delta C/\Delta C}$ mice (Figure 5C). Taken together, the results of these loss-of-function and gain-of-function experiments suggest that failure to engage upon re-exposure to a novel context specifically in *Shank3*$^{\Delta C/\Delta C}$ mice involves failure to recruit PreL→TS projection neuron activity sufficient to counteract an engagement-preventing DA-mediated memory induced in TS of *Shank3*$^{\Delta C/\Delta C}$ mice upon first exposure.

The specific requirements for activity in PreL→TS projection neurons to engage upon context re-exposure in WT and *Shank3*$^{\Delta C/\Delta C}$ mice might reflect long-term memory consolidation processes induced upon first exposure to novel context and involving PreL. Indeed, when WT mice were treated locally in PreL with D1/5R antagonist 12 h after first context exposure, engagement upon re-exposure now mimicked first exposure in that it did not depend on activity in PreL→TS projection neurons (WT Saline 212.9 ± 15.6 s, WT PreL→TS sil and D1/5 antagonist 257.6 ± 19.4 s, p = 0.2321; Figure 5D). Likewise, local treatment with D1/5R antagonist in PreL of *Shank3*$^{\Delta C/\Delta C}$ mice 12 h after first context exposure rescued engagement with conspecifics or objects upon context re-exposure to levels indistinguishable from those exhibited by WT mice (WT 185.4 ± 22.1 s, *Shank3*$^{\Delta C/\Delta C}$ 223.2 ± 22.7 s, p = 0.4244; Figure 5E). In contrast, delivery of the D1/5R antagonist locally to ACC 12 h after initial exposure did not rescue engagement in *Shank3*$^{\Delta C/\Delta C}$ mice (Figure 5E). Finally, consistent with the notion that the procedure had restored engagement in the ASD model mice by suppressing the memory of the initial exposure to novel context (i.e., day 2 effectively became again day 1 with respect to novel context exposure), when an additional re-exposure step (day 3) was added subsequent to interference with long-term memory consolidation in PreL after initial novel context exposure, *Shank3*$^{\Delta C/\Delta C}$ mice again failed to engage (Figure 5F). Therefore, exposure to a novel context induces memory consolidation processes involving PreL in both WT and *Shank3*$^{\Delta C/\Delta C}$ mice, which account for how WT and *Shank3*$^{\Delta C/\Delta C}$ mice engage at context re-exposure.

Familiarity at first context exposure prevents subsequent failure to engage in *Shank3*$^{\Delta C/\Delta C}$ mice

To investigate what might underlie the long-term memory consolidation processes involving TS and PreL of *Shank3*$^{\Delta C/\Delta C}$ mice leading to failure to engage upon context re-exposure, we hypothesized that mutant mice might differ from WT mice in how they perceive a novel context. To begin to explore this possibility, we carried out corresponding PreL (local PV neuron activation) and PreL→TS projection neuron silencing experiments during initial exposure to novel context and monitored the acute impact on engagement in WT and *Shank3*$^{\Delta C/\Delta C}$ mice (Figures 6A and S5). In WT mice, silencing PreL (*PV-Cre* mice) or PreL→TS projection neurons did not detectably affect engagement at first exposure to novel context (PreL→TS: WT Saline 236.8 ± 14.9 s, WT PreL→TS sil. 218.1 ± 9.8 s, p = 0.8245; Figures 6A and S5). In striking contrast, the same manipulations prevented engagement and induced self-centered behaviors during initial novel context exposure in *Shank3*$^{\Delta C/\Delta C}$ mice as compared with saline controls (PreL→TS: *Shank3*$^{\Delta C/\Delta C}$ Saline 197.9 ± 23.5 s, *Shank3*$^{\Delta C/\Delta C}$ PreL→TS sil. 75.2 ± 36.4 s, p = 0.0038; Figures 6A and S5). Silencing ACC or BLA did not prevent engagement at first exposure in *PV-Cre;Shank3*$^{\Delta C/\Delta C}$ mice (Figure S5). Therefore, and consistent with elevated TS DA transients (Figure 4B), *Shank3*$^{\Delta C/\Delta C}$ mice experience the first exposure to novel context different to WT mice, as revealed by a dependency on activity in PreL and PreL→TS projection neurons for engagement in *Shank3*$^{\Delta C/\Delta C}$ but not WT mice.

What aspect of novel context exposure might lead to adverse memory consolidation and subsequent failure to engage in *Shank3*$^{\Delta C/\Delta C}$ mice? Insistence on sameness is a core hallmark of ASD, prompting us to hypothesize that a novel context lacking any familiar feature might be experienced negatively by *Shank3*$^{\Delta C/\Delta C}$ mice. We reasoned that this might be offset by inclusion of familiarized objects or familiar features to the novel context at first exposure. To probe this hypothesis, we familiarized mutant mice to novel objects (Falcon tubes) by placing them in their home cage for 10 days prior to exposure to novel context in the presence of now familiarized objects. Consistent with the notion that absence of familiarity accounted for the requirement for activity in PreL to facilitate engagement at first exposure to novel context in *Shank3*$^{\Delta C/\Delta C}$ mice, silencing PreL did not affect engagement when initial exposure to novel context included a familiarized object in *PV-Cre;Shank3*$^{\Delta C/\Delta C}$ mice (*PV-Cre* 181.87 ± 20.1 s, *PV-Cre;Shank3*$^{\Delta C/\Delta C}$ 163.8 ± 15.8 s, p = 0.7446; Figure 6B).

Consistent with the notion that the induction of ASD-like phenotypes upon first exposure to a novel context in *Shank3*$^{\Delta C/\Delta C}$ mice is linked to an aversion against unfamiliarity, when initial exposure to a novel context included familiarized objects, *Shank3*$^{\Delta C/\Delta C}$ mice engaged with conspecifics at re-exposure in a way indistinguishable from WT mice (Figure 6C). This included indistinguishable levels of engagement (WT with familiarized objects 256.7 ± 16.2 s, *Shank3*$^{\Delta C/\Delta C}$ with familiarized objects 221.8 ± 21.13 s, p = 0.7075) and indistinguishable

Figure 6. Familiarity at first context exposure prevents subsequent failure to engage in *Shank3*$^{\Delta C/\Delta C}$ mice

(A and B) Engagement during first exposure. Silencing of PreL→TS projection neurons during first exposure suppresses social exploration specifically in *Shank3*$^{\Delta C/\Delta C}$ mice (A). Inclusion of familiarized object at first exposure removes dependence on PreL activity to engage in *Shank3*$^{\Delta C/\Delta C}$ mice (B).

(C) Inclusion of familiarized objects at first exposure to a novel context rescues engagement at re-exposure in *Shank3*$^{\Delta C/\Delta C}$ mice (saline, left); like in WT mice, engagement at re-exposure now depends on activity in PreL (PSEM, right). Dashed bars: values in the absence of familiarized objects (std. housing) are replotted (from Figure 5A) for comparison.

(D–F) Inclusion of fresh bedding material during first context exposure prevents engagement deficits at re-exposure (social, D; objects, E) as well as at subsequent re-exposure (day 3, F) in *Shank3*$^{\Delta C/\Delta C}$ mice.

(G) Comparable retreat-related DA transients in TS at first exposure to novel context in the presence of bedding in WT and *Shank3*$^{\Delta C/\Delta C}$ mice.

For all panels: n ≥ 5; values are means ± SEM; two-way-RM-ANOVA, Sidak's post hoc test; ns = non significant, p < 0.05 (*), p < 0.001 (**) p < 0.0001 (***); black circles (WT) and red squares (*Shank3*$^{\Delta C/\Delta C}$) indicate values from individual mice.

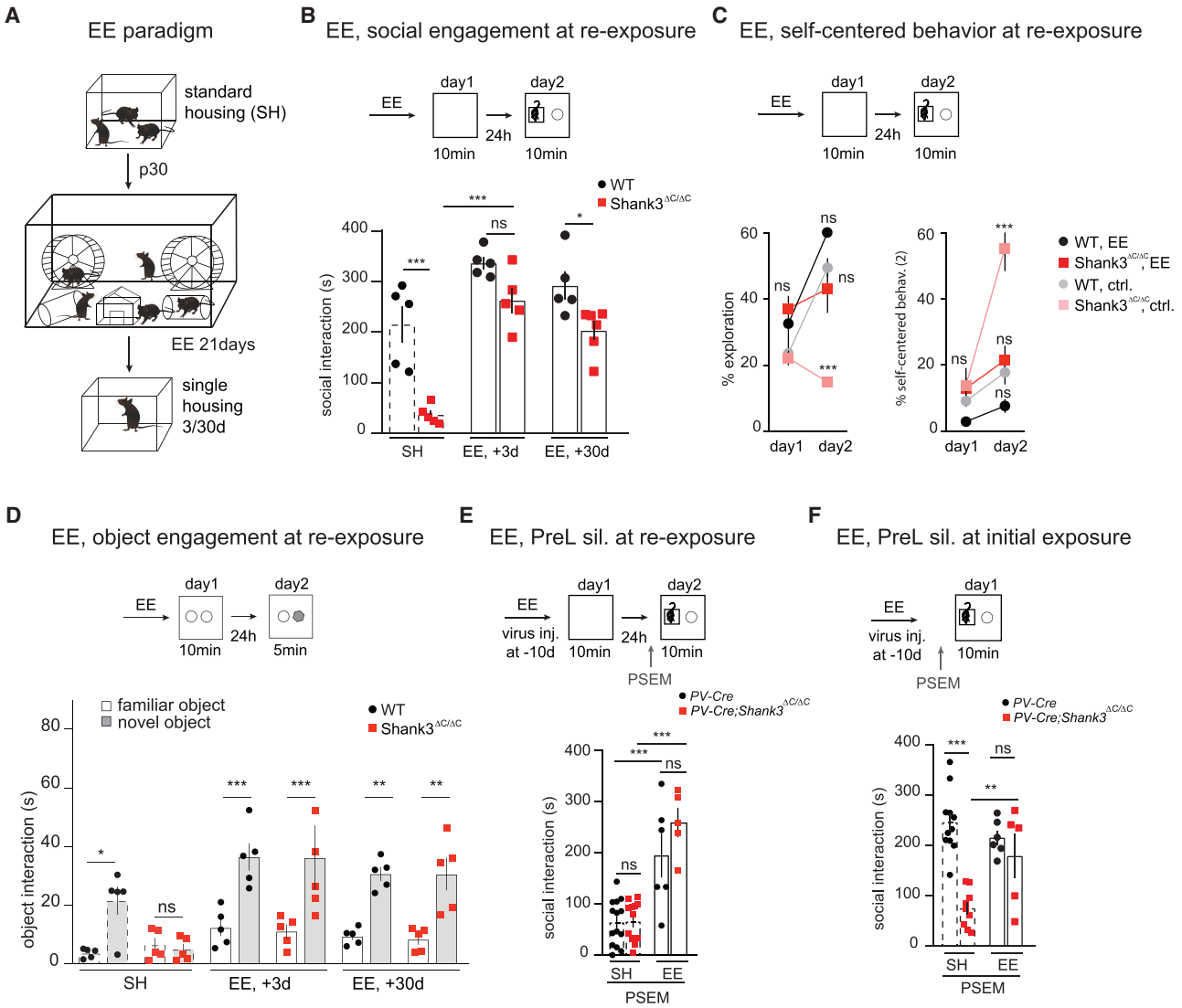

Figure 7. Environmental enrichment prevents ASD-like phenotypes and obviates requirement for PreL activity

(A) Schematic representation of the environmental enrichment (EE) protocol.

(B–D) EE long lastingly rescues social engagement deficits (B), exploration, and self-centered behaviors (C), as well as engagement toward objects (D) upon context re-exposure in *Shank3*$^{\Delta C/\Delta C}$ mice. SH: standard housing.

(E and F) EE obviates requirement for activity in PreL to facilitate engagement at re-exposure (E, WT and *Shank3*$^{\Delta C/\Delta C}$) and at first exposure to context (F, *Shank3*$^{\Delta C/\Delta C}$). Standard housing (SH) values replotted (dashed bars) for comparison.

For all panels: n ≥ 5; values are means ± SEM; two-way-RM-ANOVA, Sidak's post hoc test; ns = non significant, $p < 0.05$ (*), $p < 0.001$ (**) $p < 0.0001$ (***); black circles (WT) and red squares (*Shank3*$^{\Delta C/\Delta C}$) indicate values from individual mice.

dependences on activity in PreL→TS projection neurons at re-exposure (WT fam obj PreL sil. 111.4 ± 30.1 s, *Shank3*$^{\Delta C/\Delta C}$ fam obj PreL sil.106.2 ± 26.3 s, $p = 0.9997$; Figure 6C). The presence of the familiarized object at context re-exposure was not necessary to promote engagement (Figure 6C), indicating that its presence at first exposure was sufficient to prevent subsequent context-specific lack of engagement in the mutant mice. In control experiments, inclusion of nonfamiliar objects at initial exposure did not prevent subsequent lack of engagement or other ASD hallmarks in *Shank3*$^{\Delta C/\Delta C}$ mice (Figure S5). Consistent with the notion that the presence of a familiar feature (and not specifically of a familiar object) was the critical factor in preventing lack of engagement, addition of a small amount of fresh bedding material (i.e., material familiar to mice from their home cage) during initial exposure to novel context also completely prevented failure to engage with conspecifics (Figure 6D) or objects (Figure 6E) upon context re-exposure in *Shank3*$^{\Delta C/\Delta C}$ mice (Figure 6D). In line with the notion that the presence of familiar features prevented all aspects of context-specific failure to engage in *Shank3*$^{\Delta C/\Delta C}$ mice, like in *PV-Cre* mice, engagement upon re-exposure now again depended on activity in PreL in *PV-Cre;Shank3*$^{\Delta C/\Delta C}$ mice (Figure 6D). Notably, when fresh

bedding material was included at first exposure to novel context, *Shank3*$^{\Delta C/\Delta C}$ mice still exhibited robust engagement upon a second re-exposure on day 3, indicating that the presence of a familiar feature at first exposure to a novel context produced long-lasting WT-like engagement in that context in *Shank3*$^{\Delta C/\Delta C}$ mice (Figure 6F).

Did the inclusion of familiarity at first exposure to novel context influence DA transients in TS of *Shank3*$^{\Delta C/\Delta C}$ mice? When a small amount of fresh bedding material was included in the arena, retreat-related DA transients in *Shank3*$^{\Delta C/\Delta C}$ mice were greatly reduced and comparable with those detected in WT mice upon first exposure on day 1 (peak %dF/F WT 2.70 ± 0.94, *Shank3*$^{\Delta C/\Delta C}$ 3.85 ± 2.52, p = 0.68; Figure 6G). In parallel with engagement toward a novel object, retreat-related DA transients in *Shank3*$^{\Delta C/\Delta C}$ mice at context re-exposure in the presence of bedding were indistinguishable from those detected in WT (peak %dF/F WT 2.51 ± 1.95, *Shank3*$^{\Delta C/\Delta C}$ 2.43 ± 1.12, p = 0.32; Figure 6G). The results suggest that the elevated DA transients in TS upon novel context exposure and the subsequent failure to engage at re-exposure are induced by an aspect of novel context experience in the absence of familiarity in *Shank3*$^{\Delta C/\Delta C}$ mice.

Environmental enrichment prevents ASD-like phenotypes and obviates requirement for PreL activity

To date, successful approaches to alleviate ASD symptoms in patients involve various forms of social and environmental enrichment (EE) interventions (Aronoff et al., 2016; Hill et al., 2017; Laugeson et al., 2014; Woo et al., 2015). Understanding how these interventions lead to improved social skills is limited, but one possibility is that they might produce reduced thresholds for engagement through repeated positive reinforcement (Nithianantharajah and Hannan, 2006). To probe this model, we subjected WT and *Shank3*$^{\Delta C/\Delta C}$ mice to EE for 3 weeks (STAR Methods; Figure 7A) and investigated its impact on context-specific engagement in the absence of familiar objects or features. Remarkably, *Shank3*$^{\Delta C/\Delta C}$ mice that had undergone EE before exposure to novel context exhibited engagement toward new conspecifics (Figure 7B; WT EE3d 337.3 ± 12.0 s, *Shank3*$^{\Delta C/\Delta C}$ EE3d 263.5 ± 25.2 s, p = 0.0990; the new mice differed from those included during the EE procedure) or novel objects (Figure 7D; WT EE3d 36.45 ± 4.6 s, *Shank3*$^{\Delta C/\Delta C}$ EE3d 36.2 ± 10.9 s, p > 0.99), as well as absence of self-centered behaviors (Figure 7C) 3 days and 30 days after the enrichment protocol that were indistinguishable from WT mice. Furthermore, enriched *Shank3*$^{\Delta C/\Delta C}$ mice displayed exploratory behavior comparable with nonenriched WT mice (Figure 7C). These findings suggested that EE might be beneficial in ASD by long-lastingly promoting context-specific engagement.

To determine whether EE specifically promotes engagement in *Shank3*$^{\Delta C/\Delta C}$ mice or whether, alternatively, it might obviate a requirement for activity in PreL neurons to facilitate engagement in WT and *Shank3*$^{\Delta C/\Delta C}$ mice, we carried out corresponding PreL silencing experiments. Remarkably, silencing PreL during re-exposure did not interfere with engagement (Figure 7E) in enriched *PV-Cre* or *PV-Cre;Shank3*$^{\Delta C/\Delta C}$ mice. Furthermore, silencing PreL did not interfere with engagement during initial exposure to novel context in enriched *PV-Cre;Shank3*$^{\Delta C/\Delta C}$ mice (Figure 7F). Taken together, these results suggest that EE rescues ASD-like phenotypes in *Shank3*$^{\Delta C/\Delta C}$ mice by obviating a requirement for activity in PreL in order to engage upon first exposure and re-exposure to a novel context.

DISCUSSION

We have probed the hypothesis that failure to engage and enhancement of repetitive behaviors, core hallmarks of ASD (Chen et al., 2015; Bourgeron, 2015; Pasciuto et al., 2015), might be causally related to how a context is experienced in ASD and more specifically to aversion toward unfamiliarity, a further core hallmark of ASD (Ferhat et al., 2017; Jiujias et al., 2017). Our results reveal that ASD-like phenotypes in *Shank3*$^{\Delta C/\Delta C}$ mice are context specific, are accounted for by how mutant mice first experience a novel context and can all effectively be prevented by inclusion of familiar features at first exposure to a novel context (Figure S6). We also addressed how novel context experience might influence engagement. We demonstrate that first exposure to a novel context initiates processes involving PreL and TS in both WT and *Shank3*$^{\Delta C/\Delta C}$ mice, which determine how mice engage upon context re-exposure (Figure S6). Taken together, our results reveal how novel context experience in the absence of familiar features has a key role to trigger ASD-like phenotypes in genetically predisposed mice, linking causally a core hallmark of ASD, aversion toward unfamiliarity, to characteristic ASD-like phenotypes such as social deficits and repetitive behaviors through context-specific failure to engage.

Sameness sensitivity accounts for ASD-like phenotypes in *Shank3*$^{\Delta C/\Delta C}$ mice

Our results suggest that aversion to unfamiliarity in ASD leads to a profound deficit to engage in novel contexts first experienced in the absence of familiar items. Mechanistically, we show that together with failure to engage at subsequent re-exposure, novel context experience in the absence of familiar items induces markedly elevated retreat-related DA transients in TS specifically in *Shank3*$^{\Delta C/\Delta C}$ mice. Strikingly, inclusion of familiar features at first exposure is sufficient to prevent the elevated DA transients as well as all aspects of altered context-specific regulation of engagement in *Shank3*$^{\Delta C/\Delta C}$ mice. Our results suggest that enhanced DA transients induce plasticity in TS sufficient to produce subsequent context-specific failure to engage in *Shank3*$^{\Delta C/\Delta C}$ mice. Whether inducing elevated DA transients in TS might be sufficient to produce subsequent context-specific failure to engage in WT mice remains to be determined.

Studies evaluating social engagement using versions of the three-chamber assay have reported no impairments (Speed et al., 2015), mild impairments (Kouser et al., 2013; Wang et al., 2016; Drapeau et al., 2018), and strong impairments in *Shank3* models of ASD (Peça et al., 2011; Duffney et al., 2015; Bidinosti et al., 2016). The discrepancies were initially assigned to different types of *Shank3* mutations affecting diverse isoforms in the models, but varying findings in 6 independent models involving exon 21 deletions are not entirely consistent with this interpretation (Bidinosti et al., 2016; Duffney et al., 2015; Drapeau et al., 2018; Kouser et al., 2013; Speed et al., 2015; Wang et al., 2016). At closer examination, we note that studies

reporting strong impairments involved prehabituation to the chamber at least 24 h before testing (Duffney et al., 2015; Bidinosti et al., 2016), whereas weak phenotypes were found in studies involving habituation and testing on the same day. Furthermore, and notably, the original report to which most of the studies refer to (Moy et al., 2004) included a small amount of bedding material in the chamber. Therefore, although further differences might be important, re-exposure to a novel context lacking familiar features at least 12 h after initial exposure might account for several of the engagement differences among previous studies.

How absence of familiarity triggers enhanced DA transients in TS of *Shank3*$^{\Delta C/\Delta C}$ mice remains to be determined, but one possibility is that sensory filtering deficits and the associated hypersensitivity in ASD (Jamal et al., 2021) might result in enhanced recruitment of dopaminergic neurons in SNL that project to TS (Menegas et al., 2015). Our findings are consistent with pronounced novelty aversion in ASD patients (Gosling and Moutier, 2018), but how the mechanisms involved in *Shank3*$^{\Delta C/\Delta C}$ mice will generalize to further genetic models of autism remain to be determined.

Control of context-specific engagement involves PreL→TS projection neurons

Our findings uncover a systems-level mechanism involving PreL and PreL→TS projection neurons that supports engagement upon re-exposure to a novel context. We show that first exposure to a novel context induces long-term memory consolidation processes involving both TS and PreL, leading to engagement upon context re-exposure mediated by activity in PreL→TS projection neurons. This engagement-promoting mechanism is context specific and long lasting, providing a framework to account for how reinforcement of retreat behavior through DA release in TS by Substantia Nigra lateralis neurons (Menegas et al., 2018) is counteracted by a context-specific prefrontal mechanism (Figure S6). We hypothesize that this might work akin to a push-and-pull mechanism, in which DA transients at first exposure set the level of resistance within TS through a long-term consolidation process. Thus, our findings are consistent with and extend the notion that activity in PreL neurons can mediate context-related control of behavior (Murugan et al., 2017; Park et al., 2021; Wiltgen et al., 2004; Yizhar and Levy, 2021). In addition, they suggest that PreL→TS projection neurons act hand in hand with a memory process set in place in TS by DA signaling at first exposure to novel context.

Interestingly, and possibly due to enhanced DA transients in TS, activity in PreL→TS projection neurons was already necessary for engagement during first exposure to novel context in *Shank3*$^{\Delta C/\Delta C}$ mice. Subsequent plasticity induced in TS networks upon elevated DA transients might result in endogenous PreL→TS activity being insufficient to counteract lack of engagement upon memory consolidation. Our results relate mechanistically ASD-like phenotypes in the autism model mice to altered settings of a specific mechanism promoting context-specific engagement through PreL and PreL→TS projection neurons. Whether and how the requirement for activity in PreL→TS projection neurons of *Shank3*$^{\Delta C/\Delta C}$ mice at first context exposure might relate to adverse plasticity in TS networks influenced by PreL→TS inputs remains to be determined.

A further major finding of our study is that EE procedures obviate a requirement for activity in PreL neurons to engage in both WT and *Shank3*$^{\Delta C/\Delta C}$ mice, preventing ASD-like phenotypes in mutant mice. EE promotes plasticity in the nervous system (Renner and Rosenzweig, 1987; van Praag et al., 2000), but how exactly this relates to its multiple beneficial effects in dysfunction settings has remained poorly understood. The enrichment procedures involve repeated exposure to novelty, playful engagement with objects, enhanced social interactions, and enhanced motor activity (Nithianantharajah and Hannan, 2006; Renner and Rosenzweig, 1987; van Praag et al., 2000). Elucidating which of these aspects of EE are particularly effective in an autism setting will have important therapeutic implications.

Remarkably, the EE procedure obviated a requirement for activity in PreL neurons to facilitate engagement during first exposure to a novel context in *Shank3*$^{\Delta C/\Delta C}$ mice and had a comparable effect in WT and *Shank3*$^{\Delta C/\Delta C}$ mice to obviate a requirement for activity in PreL neurons in order to promote engagement upon context re-exposure. These striking observations suggest that rather than specifically alleviating ASD-related features such as an aversion toward unfamiliarity, EE might generally facilitate context-related engagement. Whether and how this might involve alterations in TS DA release and PreL-TS networks involved in context-related engagement remains to be determined.

Outlook

In conclusion, our results are consistent with the hypothesis that the escalation of ASD-related dysfunctions in genetically predisposed individuals could be prevented by enrichment procedures, which based on our findings are likely most effective when conducted with the consistent inclusion of familiar features in a patient's expanding world. The results of our study specifically implicate DA transients in TS and activity in PreL→TS projection neurons in the control of context-specific engagement in WT and *Shank3*$^{\Delta C/\Delta C}$ mice. However, further brain areas and their projections likely contribute to the phenotype, and our findings will serve as a starting point to investigate how interrelated brain networks influence context-related engagement in mental health.

STAR★METHODS

Detailed methods are provided in the online version of this paper and include the following:

- KEY RESOURCES TABLE
- RESOURCE AVAILABILITY
  - Lead contact
  - Materials availability
  - Data and code availability
- EXPERIMENTAL MODEL AND SUBJECT DETAILS
  - Behavioral procedures
  - Stereotaxic surgery
  - DA detection through fiber photometry in situ
  - Pharmacogenetic experiments in vivo

- Slice electrophysiology
- Pharmacology in vivo
- Histological verification of injection sites

- METHODS DETAILS
- QUANTIFICATION AND STATISTICAL ANALYSIS

SUPPLEMENTAL INFORMATION

Supplemental information can be found online at https://doi.org/10.1016/j.neuron.2022.02.001.

ACKNOWLEDGMENTS

We thank members of the Caroni group for discussions about the project. Funding: S.K. was supported by a Novartis Presidential Program Postdoctoral Fellowship; A.F. and S.A. were supported by funding from the European Research Council (ERC) under the European Union's Horizon 2020 research and innovation program (Descent, grant agreement no 692617), the Swiss National Science Foundation, the Kanton Basel-Stadt and the Novartis Research Foundation; A.F. was supported by a Biozentrum PhD Fellowship; and S.K. and P.C. were supported by the Swiss National Foundation for Research (NCCR Synapsy) and the Novartis Research Foundation (FMI).

AUTHOR CONTRIBUTIONS

S.K. and P.C. devised the study. S.K. conducted all experiments and analyses, except for the DA recording experiments and their analyses, which were conducted by A.F., and the slice recordings, which were conducted by S.V. A.F. and S.A. provided critical advise. T.B. co-mentored S.K. and provided critical inputs to the project. I.G. participated in early phases of the project and contributed the *Shank3*$^{\Delta C/\Delta C}$ mice. P.C. and S.K. wrote the manuscript.

DECLARATION OF INTERESTS

The authors declare no competing interests.

Received: July 14, 2021
Revised: January 10, 2022
Accepted: January 28, 2022
Published: February 25, 2022

REFERENCES

Aronoff, E., Hillyer, R., and Leon, M. (2016). Environmental enrichment therapy for autism: outcomes with increased access. Neural Plast *2016*, 2734915. 10.1155/2016/2734915.

Bailey, A., Palferman, S., Heavey, L., and Le Couteur, A. (1998). Autism: the phenotype in relatives. J. Autism Dev. Disord. *28*, 369–392.

Balleine, B.W., and O'Doherty, J.P. (2010). Human and rodent homologies in action control: corticostriatal determinants of goal-directed and habitual action. Neuropsychopharmacology *35*, 48–69. 10.1038/npp.2009.131.

Baron-Cohen, S., and Belmonte, M.K. (2005). Autism: a window onto the development of the social and the analytic brain. Annu. Rev. Neurosci. *28*, 109–126. 10.1146/annurev.neuro.27.070203.144137.

Baum, S.H., Stevenson, R.A., and Wallace, M.T. (2015). Behavioral, perceptual, and neural alterations in sensory and multisensory function in autism spectrum disorder. Prog. Neurobiol. *134*, 140–160.

Bey, A.L., Wang, X., Yan, H., Kim, N., Passman, R.L., Yang, Y., Cao, X., Towers, A.J., Hulbert, S.W., Duffney, L.J., et al. (2018). Brain region-specific disruption of Shank3 in mice reveals a dissociation for cortical and striatal circuits in autism-related behaviors. Transl. Psychiatr. *8*, 94. 10.1038/s41398-018-0142-6.

Bidinosti, M., Botta, P., Krüttner, S., Proenca, C.C., Stoehr, N., Bernhard, M., Fruh, I., Mueller, M., Bonenfant, D., Voshol, H., et al. (2016). CLK2 inhibition ameliorates autistic features associated with SHANK3 deficiency. Science *351*, 1199–1203. 10.1126/science.aad5487.

Bourgeron, T. (2015). For the genetic architecture to synaptic plasticity in autism spectrum disorder. Nat. Rev. Neurosci. *16*, 551–563. 10.1038/nrn3992.

Brumback, A.C., Ellwood, I.T., Kjaerby, C., Iafrati, J., Robinson, S., Lee, A.T., Patel, T., Nagaraj, S., Davatolhagh, F., and Sohal, V.S. (2018). Identifying specific prefrontal neurons that contribute to autism-associated abnormalities in physiology and social behavior. Mol. Psychiatr. *23*, 2078–2089. 10.1038/mp.2017.213.

Chen, J.A., Peñagarikano, O., Belgard, T.G., Swarup, V., and Geschwind, D.H. (2015). The emerging picture of autism spectrum disorder: genetics and pathology. Annu. Rev. Pathol. *10*, 111–144. 10.1146/annurev-pathol-012414-040405.

Chen, Q., Deister, C.A., Gao, X., Guo, B., Lynn-Jones, T., Chen, N., Wells, M.F., Liu, R., Goard, M.J., Dimidschstein, J., et al. (2020). Dysfunction of cortical GABAergic neurons leads to sensory hyper-reactivity in a Shank3 mouse model of ASD. Nat. Neurosci. *23*, 520–532. 10.1038/s41593-020-0598-6.

Drapeau, E., Riad, M., Kajiwara, Y., and Buxbaum, J.D. (2018). Behavioral phenotyping of an improved mouse model of Phelan-McDermid syndrome with a complete deletion of the Shank3 gene. eNeuro *5*. 10.1523/ENEURO.0046-18.2018.

Duffney, L.J., Zhong, P., Wei, J., Matas, E., Cheng, J., Qin, L., Ma, K., Dietz, D.M., Kajiwara, Y., Buxbaum, J.D., and Yan, Z. (2015). Autism-like deficits in Shank3-deficient mice are rescued by targeting actin regulators. Cell Rep *11*, 1400–1413. 10.1016/j.celrep.2015.04.064.

Durand, C.M., Betancur, C., Boeckers, T.M., Bockmann, J., Chaste, P., Fauchereau, F., Nygren, G., Rastam, M., Gillberg, I.C., Anckarsäter, H., et al. (2007). Mutations in the gene encoding the synaptic scaffolding protein SHANK3 are associated with autism spectrum disorders. Nat. Genet. *39*, 25–27. 10.1038/ng1933.

Fenno, L.E., Mattis, J., Ramakrishnan, C., Hyun, M., Lee, S.Y., He, M., Tucciarone, J., Selimbeyoglu, A., Berndt, A., Grosenick, L., et al. (2014). Targeting cells with single vectors using multiple-feature Boolean logic. Nat. Methods *11*, 763–772. 10.1038/nmeth.2996.

Ferhat, A.T., Halbedl, S., Schmeisser, M.J., Kas, M.J., Bourgeron, T., and Ey, E. (2017). Behavioural phenotypes and neural circuit dysfunctions in mouse models of autism spectrum disorder. Adv. Anat. Embryol. Cell Biol. *224*, 85–101. 10.1007/978-3-319-52498-6_5.

Gauthier, J., Spiegelman, D., Piton, A., Lafrenière, R.G., Laurent, S., St-Onge, J., Lapointe, L., Hamdan, F.F., Cossette, P., Mottron, L., et al. (2009). Novel de novo SHANK3 mutation in autistic patients. Am. J. Med. Genet. B Neuropsychiatr. Genet. *150B*, 421–424. 10.1002/ajmg.b.30822.

Gerfen, C.R., and Surmeier, D.J. (2011). Modulation of striatal projection systems by dopamine. Annu. Rev. Neurosci. *34*, 441–466. 10.1146/annurev-neuro-061010-113641.

Geschwind, D.H. (2009). Advances in autism. Annu. Rev. Med. *60*, 367–380. 10.1146/annurev.med.60.053107.121225.

Gosling, C.J., and Moutier, S. (2018). Brief report: risk-aversion and rationality in autism spectrum disorders. J. Autism Dev. Disord. *48*, 3623–3628. 10.1007/s10803-018-3616-8.

Guo, B., Chen, J., Chen, Q., Ren, K., Feng, D., Mao, H., Yao, H., Yang, J., Liu, H., Liu, Y., et al. (2019). Anterior cingulate cortex dysfunction underlies social deficits in Shank3 mutant mice. Nat. Neurosci. *22*, 1223–1234. 10.1038/s41593-019-0445-9.

Hill, T.L., Gray, S.A.O., Baker, C.N., Boggs, K., Carey, E., Johnson, C., Kamps, J.L., and Varela, R.E. (2017). A pilot study examining the effectiveness of the PEERS Program on social skills and anxiety in adolescents with autism spectrum disorder. J. Dev. Phys. Disabil. *29*, 797–808. 10.1007/s10882-017-9557-x.

Jamal, W., Cardinaux, A., Haskins, A.J., Kjelgaard, M., and Sinha, P. (2021). Reduced sensory habituation in autism and its correlation with behavioral

measures. J. Autism Dev. Disord. *51*, 3153–3164. 10.1007/s10803-020-04780-1.

Jaramillo, T.C., Speed, H.E., Xuan, Z., Reimers, J.M., Liu, S., and Powell, C.M. (2016). Altered striatal synaptic function and abnormal behaviour in Shank3 exon4-9 deletion mouse model of autism. Autism Res *9*, 350–375. 10.1002/aur.1529.

Jaramillo, T.C., Xuan, Z., Reimers, J.M., Escamilla, C.O., Liu, S., and Powell, C.M. (2020). Early restoration of Shank3 expression in Shank3 knock-out mice prevents core ASD-like behavioral phenotypes. eNeuro *7*. 10.1523/ENEURO.0332-19.2020.

Jiang, H., and Kim, H.F. (2018). Anatomical inputs from the sensory and value structures to the tail of the rat striatum. Front. Neuroanat. *12*, 30. 10.3389/fnana.2018.00030.

Jiujias, M., Kelley, E., and Hall, L. (2017). Restricted, repetitive behaviors in autism spectrum disorder and obsessive-compulsive disorder: a comparative review. Child Psychiatr. Hum. Dev. *48*, 944–959. 10.1007/s10578-017-0717-0.

Karunakaran, S., Chowdhury, A., Donato, F., Quairiaux, C., Michel, C.M., and Caroni, P. (2016). PV plasticity sustained through D1/5 dopamine signaling required for long-term memory consolidation. Nat. Neurosci. *19*, 454–464. 10.1038/nn.4231.

Katche, C., Cammarota, M., and Medina, J.H. (2013). Molecular signatures and mechanisms of long-lasting memory consolidation and storage. Neurobiol. Learn. Mem. *106*, 40–47.

Kouser, M., Speed, H.E., Dewey, C.M., Reimers, J.M., Widman, A.J., Gupta, N., Liu, S., Jaramillo, T.C., Bangash, M., Xiao, B., et al. (2013). Loss of predominant Shank3 isoforms results in hippocampus-dependent impairments in behavior and synaptic transmission. J. Neurosci. *33*, 18448–18468. 10.1523/JNEUROSCI.3017-13.2013.

Krüttner, S., Traunmüller, L., Dag, U., Jandrasits, K., Stepien, B., Iyer, N., Fradkin, L.G., Noordermeer, J.N., Mensh, B.D., and Keleman, K. (2015). Synaptic Orb2A bridges memory acquisition and late memory consolidation in Drosophila. Cell Rep *11*, 1953–1965. 10.1016/j.celrep.2015.05.037.

Laugeson, E.A., Ellingsen, R., Sanderson, J., Tucci, L., and Bates, S. (2014). The ABC's of teaching social skills to adolescents with autism spectrum disorder in the classroom: the UCLA PEERS (®) Program. J. Autism Dev. Disord. *44*, 2244–2256. 10.1007/s10803-014-2108-8.

Lee, J., Chung, C., Ha, S., Lee, D., Kim, D.Y., Kim, H., and Kim, E. (2015). Shank3-mutant mice lacking exon 9 show altered excitation/inhibition balance, enhanced rearing, and spatial memory deficit. Front. Cell. Neurosci. *9*, 94. 10.3389/fncel.2015.00094.

Leekam, S.R., Nieto, C., Libby, S.J., Wing, L., and Gould, J. (2007). Describing the sensory abnormalities of children and adults with autism. J. Autism Dev. Disord. *37*, 894–910. 10.1007/s10803-006-0218-7.

Levy, D.R., Tamir, T., Kaufman, M., Parabucki, A., Weissbrod, A., Schneidman, E., and Yizhar, O. (2019). Dynamics of social representation in the mouse prefrontal cortex. Nat. Neurosci. *22*, 2013–2022. 10.1038/s41593-019-0531-z.

Magnus, C.J., Lee, P.H., Atasoy, D., Su, H.H., Looger, L.L., and Sternson, S.M. (2011). Chemical and genetic engineering of selective ion channel-ligand interactions. Science *333*, 1292–1296. 10.1126/science.1206606.

Mei, Y., Monteiro, P., Zhou, Y., Kim, J.A., Gao, X., Fu, Z., and Feng, G. (2016). Adult restoration of Shank3 expression rescues selective autistic-like phenotypes. Nature *530*, 481–484. 10.1038/nature16971.

Menegas, W., Akiti, K., Amo, R., Uchida, N., and Watabe-Uchida, M. (2018). Dopamine neurons projecting to the posterior striatum reinforce avoidance of threatening stimuli. Nat. Neurosci. *21*, 1421–1430. 10.1038/s41593-018-0222-1.

Menegas, W., Bergan, J.F., Ogawa, S.K., Isogai, Y., Umadevi Venkataraju, K., Osten, P., Uchida, N., and Watabe-Uchida, M. (2015). Dopamine neurons projecting to the posterior striatum form an anatomically distinct subclass. Elife *4*, e10032. 10.7554/eLife.10032.

Moessner, R., Marshall, C.R., Sutcliffe, J.S., Skaug, J., Pinto, D., Vincent, J., Zwaigenbaum, L., Fernandez, B., Roberts, W., Szatmari, P., and Scherer, S.W. (2007). Contribution of SHANK3 mutations to autism spectrum disorder. Am. J. Hum. Genet. *81*, 1289–1297. 10.1086/522590.

Monteiro, P., and Feng, G. (2017). SHANK proteins: roles at the synapse and in autism spectrum disorder. Nat. Rev. Neurosci. *18*, 147–157. 10.1038/nrn.2016.183.

Moy, S.S., Nadler, J.J., Perez, A., Barbaro, R.P., Johns, J.M., Magnuson, T.R., Piven, J., and Crawley, J.N. (2004). Sociability and preference for social novelty in five inbred strains: an approach to assess autistic-like behavior in mice. Genes Brain Behav *3*, 287–302. 10.1111/j.1601-1848.2004.00076.x.

Murugan, M., Jang, H.J., Park, M., Miller, E.M., Cox, J., Taliaferro, J.P., Parker, N.F., Bhave, V., Hur, H., Liang, Y., et al. (2017). Combined social and spatial coding in a descending projection from the prefrontal cortex. Cell *171*, 1663–1677, e16. 10.1016/j.cell.2017.11.002.

Nithianantharajah, J., and Hannan, A.J. (2006). Enriched environments, experience-dependent plasticity and disorders of the nervous system. Nat. Rev. Neurosci. *7*, 697–709. 10.1038/nrn1970.

Orefice, L.L., Mosko, J.R., Morency, D.T., Wells, M.F., Tasnim, A., Mozeika, S.M., Ye, M., Chirila, A.M., Emanuel, A.J., Rankin, G., et al. (2019). Targeting peripheral somatosensory neurons to Improve tactile-related phenotypes in ASD models. Cell *178*, 867–886, e24. 10.1016/j.cell.2019.07.024.

Orefice, L.L., Zimmerman, A.L., Chirila, A.M., Sleboda, S.J., Head, J.P., and Ginty, D.D. (2016). Peripheral mechanosensory neuron dysfunction underlies tactile and behavioral deficits in mouse models of ASDs. Cell *166*, 299–313. 10.1016/j.cell.2016.05.033.

Park, A.J., Harris, A.Z., Martyniuk, K.M., Chang, C.Y., Abbas, A.I., Lowes, D.C., Kellendonk, C., Gogos, J.A., and Gordon, J.A. (2021). Reset of hippocampal-prefrontal circuitry facilitates learning. Nature *591*, 615–619. 10.1038/s41586-021-03272-1.

Pasciuto, E., Borrie, S.C., Kanellopoulos, A.K., Santos, A.R., Cappuyns, E., D'Andrea, L., Pacini, L., and Bagni, C. (2015). Autism spectrum disorders: translating human deficits into mouse behavior. Neurobiol. Learn. Mem. *124*, 71–87. 10.1016/j.nlm.2015.07.013.

Patriarchi, T., Cho, J.R., Merten, K., Howe, M.W., Marley, A., Xiong, W.-H., Folk, R.W., Broussard, G.J., Liang, R., Jang, M.J., et al. (2018). Ultrafast neuronal imaging of dopamine dynamics with designed genetically encoded sensors. Science *360*, eeat4422.

Peça, J., Feliciano, C., Ting, J.T., Wang, W., Wells, M.F., Venkatraman, T.N., Lascola, C.D., Fu, Z., and Feng, G. (2011). Shank3 mutant mice display autistic-like behaviours and striatal dysfunction. Nature *472*, 437–442. 10.1038/nature09965.

Peixoto, R.T., Chantranupong, L., Hakim, R., Levasseur, J., Wang, W., Merchant, T., Gorman, K., Budnik, B., and Sabatini, B.L. (2019). Abnormal striatal development underlies the early onset of behavioral deficits in Shank3B(−/−) mice. Cell Rep *29*, 2016–2027, e4. 10.1016/j.celrep.2019.10.021.

Peixoto, R.T., Wang, W., Croney, D.M., Kozorovitskiy, Y., and Sabatini, B.L. (2016). Early hyperactivity and precocious maturation of corticostriatal circuits in Shank3B(−/−) mice. Nat. Neurosci. *19*, 716–724. 10.1038/nn.4260.

Phelan, K., and McDermid, H.E. (2012). The 22q13.3 deletion syndrome (Phelan-McDermid syndrome). Mol. Syndromol. *2*, 186–201.

Pisula, E., and Ziegart-Sadowska, K. (2015). Broader autism phenotype in siblings of children with ASD—a review. Int. J. Mol. Sci. *16*, 13217–13258. 10.3390/ijms160613217.

Renner, M.J., and Rosenzweig, M.R. (1987). Enriched and Impoverished Environments: Effects on Brain and Behaviour (Springer).

Robertson, C.E., and Baron-Cohen, S. (2017). Sensory perception in autism. Nat. Rev. Neurosci. *18*, 671–684. 10.1038/nrn.2017.112.

Rodriguez, N.M., and Thompson, R.H. (2015). Behavioral variability and autism spectrum disorder. J. Appl. Behav. Anal. *48*, 167–187. 10.1002/jaba.164.

Ronald, A., and Hoekstra, R.A. (2011). Autism spectrum disorders and autistic traits: a decade of new twin studies. Am. J. Med. Genet. B Neuropsychiatr. Genet. *156B*, 255–274. 10.1002/ajmg.b.31159.

Rossato, J.I., Bevilaqua, L.R., Izquierdo, I., Medina, J.H., and Cammarota, M. (2009). Dopamine controls persistence of long-term memory storage. Science *325*, 1017–1020. 10.1126/science.1172545.

Sahin, M., and Sur, M. (2015). Genes, circuits, and precision therapies for autism and related neurodevelopmental disorders. Science *350*, aab3897. 10.1126/science.aab3897.

Schroeder, J.C., Reim, D., Boeckers, T.M., and Schmeisser, M.J. (2017). Genetic animal models for autism spectrum disorder. Curr. Top. Behav. Neurosci. *30*, 311–324. 10.1007/7854_2015_407.

Speed, H.E., Kouser, M., Xuan, Z., Liu, S., Duong, A., and Powell, C.M. (2019). Apparent genetic rescue of adult Shank3 exon 21 insertion mutation mice tempered by appropriate control experiments. eNeuro *6*. 10.1523/ENEURO.0317-19.2019.

Speed, H.E., Kouser, M., Xuan, Z., Reimers, J.M., Ochoa, C.F., Gupta, N., Liu, S., and Powell, C.M. (2015). Autism-associated insertion mutation (InsG) of Shank3 exon 21 causes impaired synaptic transmission and behavioral deficits. J. Neurosci. *35*, 9648–9665. 10.1523/JNEUROSCI.3125-14.2015.

Takeuchi, M., Hata, Y., Hirao, K., Toyoda, A., Irie, M., and Takai, Y. (1997). SAPAPs. A family of PSD-95/SAP90-associated proteins localized at postsynaptic density. J. Biol. Chem. *272*, 11943–11951. 10.1074/jbc.272.18.11943.

Valjent, E., and Gangarossa, G. (2021). The tail of the striatum: from anatomy to connectivity and function. Trends Neurosci *44*, 203–214. 10.1016/j.tins.2020.10.016.

van Praag, H., Kempermann, G., and Gage, F.H. (2000). Neural consequences of environmental enrichment. Nat. Rev. Neurosci. *1*, 191–198. 10.1038/35044558.

Wang, X., Bey, A.L., Katz, B.M., Badea, A., Kim, N., David, L.K., Duffney, L.J., Kumar, S., Mague, S.D., Hulbert, S.W., et al. (2016). Altered mGluR5-Homer scaffolds and corticostriatal connectivity in a Shank3 complete knockout model of autism. Nat. Commun. *7*, 11459. 10.1038/ncomms11459.

Wiltgen, B.J., Brown, R.A., Talton, L.E., and Silva, A.J. (2004). New circuits for old memories: the role of the neocortex in consolidation. Neuron *44*, 101–108. 10.1016/j.neuron.2004.09.015.

Woo, C.C., Donnelly, J.H., Steinberg-Epstein, R., and Leon, M. (2015). Environmental enrichment as a therapy for autism: a clinical trial replication and extension. Behav. Neurosci. *129*, 412–422. 10.1037/bne0000068.

Woon, E.P., Sequeira, M.K., Barbee, B.R., and Gourley, S.L. (2020). Involvement of the rodent prelimbic and medial orbitofrontal cortices in goal-directed action: a brief review. J. Neurosci. Res. *98*, 1020–1030. 10.1002/jnr.24567.

Yang, M., Bozdagi, O., Scattoni, M.L., Wöhr, M., Roullet, F.I., Katz, A.M., Abrams, D.N., Kalikhman, D., Simon, H., Woldeyohannes, L., et al. (2012). Reduced excitatory neurotransmission and mild autism-relevant phenotypes in adolescent Shank3 null mutant mice. J. Neurosci. *32*, 6525–6541. 10.1523/JNEUROSCI.6107-11.2012.

Yizhar, O., and Levy, D.R. (2021). The social dilemma: prefrontal control of mammalian sociability. Curr. Opin. Neurobiol. *68*, 67–75. 10.1016/j.conb.2021.01.007.

STAR★METHODS

KEY RESOURCES TABLE

REAGENT or RESOURCE	SOURCE	IDENTIFIER
Antibodies		
Rabbit anti-Tyrosine Hydroxylase	EMD Millipore	AB152
Rabbit anti Parvalbumin	Swant	PV27
donkey anti rabbit Alexa 647	Invitrogen	A31573
Bacterial and Virus Strains		
rAAV9-CAG-flox-PSAM (Leu41Phe,Tyr115Phe)5HT3-WPRE	Vector Biosystems Inc	N/A
AAV9-CBA-FLEX-PSAM(Leu141Phe, Tyr115Phe)GlyR-WPRE	Vector Biosystems Inc	N/A
rgAAV-Ef1a-mCherry-IRES-Cre	Fenno et al. (2014)	Addgene viral prep # 55632-AAVrg
retroAAVCre-H2BGFP	FMI vector core	N/A
pAAV9-pCAG-FLEX-SynGFPreverse-WPRE	FMI vector core	N/A
pAAV9-hSyn1-chl-dLight1.3b-WPRE-bGHp(A)	Patriarchi et al. (2018)	Addgene viral prep # 135762-AAV9
pAAV9-pCAG-FLEX-ReaChR-eYFP	FMI vector core	N/A
Chemicals, Peptides, and Recombinant Proteins		
SCH23390 hydrochloride	Tocris Bioscience	Cat#: 0925/10
PSEM308	Apex Scientific	N/A
Bungarotoxin, Alexa488 conjugate	Thermo Fisher Scientific	Cat#: B13422
desipramine	Sigma-Aldrich	D3900-1G
Pargyline	Sigma-Aldrich	P8013-500MG
6-hydroxydopamine	Sigma-Aldrich	H116-5MG
ascorbic acid	Sigma-Aldrich	PHR1008-2G
Experimental Models: Organisms/Strains		
Mouse: PV-Cre: 129P2-Pvalbtm1(cre) Arbr/J	The Jackson Laboratory	Cat#. 008069
Mouse: B6-Shank3TM1NPA	Novartis Pharma AG	N/A
Software and Algorithms		
GraphPad Prism 8	GraphPad software	https://www.graphpad.com/scientific-software/RRID:SCR_002798
ZEN2010	Carl Zeiss AG	https://www.zeiss.com/microscopy/int/products/microscope-software/zen.html
FIJI/ImageJ 1.53.c	Biobserve	https://imagej.nih.gov/ij
EthoVision XT	Noldus	https://www.noldus.com/ethovision RRID:SCR_000441

RESOURCE AVAILABILITY

Lead contact

Further information and requests for resources and reagents should be directed to and will be fulfilled by the lead contact, Pico Caroni (Pico.Caroni@fmi.ch)

Materials availability

This study did not generate new unique reagents.

Data and code availability

All data and analyses necessary to understand and assess the conclusions of the manuscript are presented in the main text and in the supplemental information. All data available upon request.

EXPERIMENTAL MODEL AND SUBJECT DETAILS

Shank3 mutant mice were as described (Bidinosti et al., 2016). Shank3 encodes a post-synaptic scaffold protein that regulates synaptic development, function and plasticity by orchestrating the assembly of postsynaptic density macromolecular signaling complexes (Monteiro and Feng, 2017; Takeuchi et al., 1997). Consistent with a function of Shank3 in controlling neuronal plasticity, recent studies suggested that adult restoration of *Shank3* can revert ASD phenotypes (Guo et al., 2019; Jaramillo et al., 2020; Mei et al., 2016; Orefice et al., 2019; Speed et al., 2019). Several studies using *Shank3* mutant mice have linked structural and functional alterations of the neocortex, the striatum and ventral hippocampus to disruption of *Shank3* function (Bey et al., 2018; Chen et al., 2020; Duffney et al., 2015; Jaramillo et al., 2016; Kouser et al., 2013; Lee et al., 2015; Peça et al., 2011; Peixoto et al., 2019, 2016; Speed et al., 2015; Wang et al., 2016; Yang et al., 2012).

The *Shank3*$^{\Delta C/\Delta C}$ mice used in this study lack exon 21 (Bidinosti et al., 2016; see also Kouser et al., 2013; Duffney et al., 2015), leading to loss of the major *Shank3* isoforms expressed in the brain; the remaining N-terminal isoforms were previously detected in brain lysates but not in synaptosomal fractions (Duffney et al., 2015). Briefly, to generate *Shank3* exon 21-deleted mice, the exon 21 genomic region of *Shank3* (2464bp in size) was replaced by homologous recombination with a loxP-TK_Neo-loxP cassette. The Neo cassette was flanked by a 3kb 5′ homology arm and a 1.6kb 3′ homology arm. Targeted ES clones were used for blastocyst injection, and chimeric males were mated with transgenic Cre-expressing C57Bl/6 mice females to remove the neomycin resistance cassette. Animals without the neo cassette were used as F1 mice to establish the *Shank3* exon 21-deleted (*Shank3*$^{\Delta C/\Delta C}$) colony.

In general, het/het breeding schemes were used to gain *Shank3*$^{\Delta C/\Delta C}$ and *Shank3*$^{+/+}$ littermates for experimental animals. Due to the lower than Mendelian ratio of pups homozygous mutant surviving this was occasionally changed to hom/hom breeding. These breeding's were established independently out of the original het/het breeding's for both *Shank3*$^{\Delta C/\Delta C}$ and *Shank3*$^{+/+}$. Although this was not statistically tested, we did not observe any obvious difference for the tests performed within this manuscript between these breeding schemes.

Heterozygous female animals were backcrossed frequently (every 6 months) to C57Bl/6 males for maintenance. Animals were weaned at 4 to 5 weeks due to their small body size.

PV-Cre mice (*129P2-Pvalbtm1 (Cre)Arbr/J*) mice were from Jackson laboratories; two independent crosses of homozygous *Shank3*$^{\Delta C/\Delta C}$ females were crossed with *PV-Cre* males. Resulting *PV-Cre;Shank3*$^{+/\Delta C}$ litters were used as founders to generate *PV-Cre*;*Shank3*$^{\Delta C/\Delta C}$ mice. Similar to the breeding scheme of *Shank3*$^{\Delta C/\Delta C}$ mutant animals, this was occasionally changed to homozygous *PV-Cre;Shank3*$^{\Delta C/\Delta C}$ and *PV-Cre;Shank3*$^{+/+}$ breeding.

Behavioral procedures

All mice were kept in type III closed-lid standard cages in temperature-controlled rooms on a constant 12-h light-dark cycle, and all experiments were conducted at approximately the same time of the light cycle (9:00 a.m-1pm). Before the behavioral experiment, mice were housed individually for 3–4 days, and provided with food and water ad libitum. No handling, except for routine cage changes once per week were performed on animals prior to the behavioral experiments or injection of AAV-virus. Before behavioral tests, animals were acclimatized to the behavior room for a minimum of 30 minutes. All experimental arenas/contexts were placed within a sound proof box equipped with camera and illumination systems to ensure consistent conditions throughout all experiments without unforeseen disturbance or variations from the surrounding. For behavioral experiments, animals were carefully taken out of their home cage and transported on the arm of the experimenter to the testing arena to minimize stress to the animals. After the behavioral procedure, animals were allowed to voluntarily climb on the lid of their home cage and transferred back to their home cage. With the occasional exception of object and social memory tasks (animals used first in object memory tasks prior to a social task), no animal was reused for several tasks in this study. All behavioral experiments were carried out with mice aged from 2 to 3 months.

All animal procedures were approved and performed in accordance with the Veterinary Department of the Kanton Basel-Stadt.

In **object recognition tasks**, mice explored two identical objects (50ml Falcon tubes) placed in a 30x50cm rectangular arena (10min exploration) on Day 1, were returned to their home cage immediately after training, and were tested for familiar object recognition 1h (short-term memory, STM) or 24h memory (long-term memory, LTM) later. For the object recognition test, one of the two objects was replaced with a new one (50 ml water bottle or cylinder filled with confetti, 5min exploration). To avoid discrimination of the objects based on odor, both the arena and the objects were thoroughly wiped with 70% ethanol before and after each trial. Only direct sniffing contact towards the objects was counted as interaction.

In **social interaction tests**, animals were allowed to explore an empty rectangular arena (30x50cm) for 10min, and returned back to their home cage. At the indicated time points (1h, 3h, 24h) animals were placed back to either the identical arena or a novel arena in which they were presented with a novel object and an intruder animal (6-8weeks old wildtype; not previous littermate) shielded inside a cage. Only direct sniffing contact towards the cage was counted as interaction.

Repetitive behavior was measured as time during which animals did not move their hind paws and displayed protracted bouts of either self-grooming, or exhibiting stereotypic circling, forward, backward or sideward movements, or were sitting and only moving their head. Exploratory behavior was measured as time during which animals actively approached objects or con-specifics by direct sniffing, or approached the walls of the arena by foraging behavior.

In **social recognition tasks**, animals were allowed to explore an empty rectangular arena (30x50cm) for 10min. Subsequently, mice were returned to their home cage for 1h, and then returned to the previous arena (5min), which now included a male intruder mouse (6-8weeks old wildtype; not previous littermate) shielded inside a cage. At the timepoints indicated following the first encounter to an intruder, interactions towards a cage harboring either the same (M1) or a novel intruder (M2) were monitored. Only direct sniffing contact towards the cage was counted as interaction.

To **familiarize animals to novel objects**, two 50ml Falcon tubes were placed upward within the home cage of the animals 10 days prior to behavioral testing. During behavioral testing, novel 50ml Falcon tubes were used within the testing arena to avoid odor pollution.

For **enriched environment** (EE) experiments, male mice were housed in groups of four to five littermates in large (rat) cages equipped with three running wheels per cage, toys, and hiding spaces. Toys and running wheels were frequently (every 4 to 7 days) replaced by novel and different toys or running wheels. Control mice were male littermates (four to five), which were housed individually in small standard cages without special equipment. Unless stated otherwise, EE was started at 1 month of age and lasted 21 days.

An **elevated plus maze** was used to monitor anxiety-like behavior. The apparatus was 52 cm in width and 50 cm in height, and was sub-divided into four arms, two of which without (open arms), and two with wall enclosures (closed arms). The open arms were illuminated by high light levels (600–700 lux). Time spent in each arm, and numbers of entries to each arm were monitored.

Stereotaxic surgery

All surgeries were conducted under aseptic conditions using a small animal stereotaxic instrument (David Kopf Instruments). Mice were anaesthetized with isoflurane using an OXYMAT3 (4% for induction, 1.5–2.0% afterward) in the stereotaxic frame for the entire surgery, and body temperature was maintained with a heating pad. Local drug treatments or viruses were delivered using glass pipettes (Drummond Scientific Company, Wiretrol II, CatNo 5-000-2005) connected to a pico spritzer (Parker Hannifin Corporation). Coordinates relative to bregma were as follows: BLA (AP −1.7, ML ± 3.2, DV −3.5 maximum volume, 200nl per injection), PreL (+1.9, ML ± 0.4, DV −2.1 maximum volume 50nl per injection), ACC (+1.0, ML ± 0.5, DV −1.2 maximum volume, 100nl per injection), TS (-1.0, ML ± 3.20, DV −2.5- 2.9 maximum volume, 200nl per injection). For drug injections, the needle was slowly lowered to 0.1 mm beyond the required DV coordinate and quickly pulled up to the original coordinate to create a pocket for injection of the drug. This prevented backflow of the drug and undesired spread into neighboring areas. Drugs were injected at the rate of 100 nl/min to the final maximum volume. After completion of the injection, the needle was left in its place for 10 min to allow for diffusion of the drug and then slowly withdrawn. All drugs and viruses were injected bilaterally in PreL, BLA, ACC and TS if not otherwise stated. Postsurgical recovery was monitored daily until the start of behavioral protocols. All injections were paired with saline injected control animals to account for any effect due to tissue damage or surgical procedure.

DA detection through fiber photometry in situ

For fibre photometry recordings, pAAV9-hSyn1-chI-dLight1.3b-WPRE-bGHp(A) (Addgene #135762) was bilaterally injected in the TS and subsequently an optic fibre was implanted 100 μm above the injection site (diameter of 200 μm, MFC_200/230-0.48_6mm_ZF1.25_FLT Mono Fibreoptic Cannula; Doric lenses). For testing experiments an additional injection of pAAV9-pCAG-FLEX-ReaChR-eYFP was delivered into the Substantia Nigra pars lateralis of DAT-Cre mice (Menegas et al., 2015) and then the same optic fiber implanted 100 μm above the injection site.

Fiber photometry recordings of dLight1.3b were started two weeks after surgery, using a multi-fibre photometry system (CineLyzer, Plexon). Implants were connected to the system through a dual branching patch cord (Plexon) to simultaneously allow for delivery of excitation light (470 nm) and collection of dLight1.3b emission at 60 Hz. A continuous excitation intensity of 30–40 μW was used.

The analysis of fibre photometric data and relative behavior was carried out using custom code in Python. Fluorescence traces at 60 frames per second obtained from the Plexon Cynelyzer system were detrended with a fitted second degree polynomial. dF/F was calculated point by point as $(signal - trend / trend)$ and multiplied by 100 to obtain percentage values. Percentage dF/F was then filtered using a Savitzky-Golay filter with a third degree polynomial and windows of 51 elements. No filtering was applied for dLight1.3b testing with dopamine neuron stimulation. Distance of the mouse from the object was computed as the distance between the center of body-mass of the mouse and object position. Obtained values were then inverted to have approaches as positive peaks and retreat events were detected using the find_peaks function from SciPy. Fluorescence traces were studied in relationship with retreat events. To compare dLight1.3b fluorescence intensity between WT and *Shank3*$^{\Delta C/\Delta C}$ mice the maximum intensity of the mean trace across trials for each mouse was computed. Obtained values were compared using a one-sided Wilcoxon rank-sum test. For peak decay analysis, maximum fluorescence intensity was calculated during each approach-retreat event in a centered window of four seconds for each mouse. Normalized peak height was obtained by dividing peak intensity by the maximum intensity displayed in that mouse. Secondly a linear model was fit onto the logarithm of peak height to obtain an exponential fit of the data with

a single coefficient and an intercept. Coefficient and intercepts were then used to calculate average decay profiles across mice and their standard error.

Pharmacogenetic experiments in vivo

Floxed PSAM-carrying AAV9 (excitation, pAAV(9)-pCAG-flox-PSAM(Leu41Phe,Tyr116Phe)5HT3-WPRE (Vector Biosystems Inc) was delivered bilaterally in *Shank3*$^{\Delta C/\Delta C;PV\text{-}Cre}$ and *Shank3*$^{+/+;PV-Cre}$ mice for acute silencing of target brain areas (Magnus et al., 2011).

For tracing experiments, a retrovirus expressing GFP (retroAAVCre-H2BGFP, FMI vector core) or a combination of retroAAV-Ef1a-mCherry-IRES-Cre (Addgene 55632-AAVrg) and a floxed synaptophysin-GFP AAV9 (pAAV9-pCAG-FLEX-SynGFPreverse-WPRE, FMI vector core) were delivered unilaterally to TS and PreL respectively.

For silencing or activation of projection neurons, floxed PSAM-carrying AAV9 (inhibition: rAAV9-CBA-flox-PSAM(Leu141Phe, Tyr116Phe)GlyR-WPRE, Vector Biosystems Inc) or (excitation, pAAV(9)-pCAG-flox-PSAM(Leu41Phe,Tyr116Phe)5HT3-WPRE (Vector Biosystems Inc) was delivered bilaterally to the indicated area (PreL, ACC, BLA), and a retro AAV delivering the Cre recombinase (rgAAV-Ef1a-mCherry-IRES-Cre, Addgene 55632-AAVrg) was delivered bilaterally to TS or DMS of the same animals.

To allow for transgene expression and its detection, mice were kept under control conditions for 10 d (28d for tracing involving synaptophysin) before any behavioral experiment. PSEM308 channel agonist (ligand, Apex Scientific) was injected intraperitoneal at 5 mg per kg of animal weight. All silencing or activation injections were carried out 20 min before the start of the behavioral procedure.

Slice electrophysiology

To assess the reduction in the excitability of pyramidal neurons upon genetic activation of PV cells, PV-Cre mice were injected in PreL with 25-50 nl of PSAM activator AAV.14 days post AAV injections, animals were anesthetized under isoflurane and perfused with 7-8 ml of ice-cold NMDG-based ACSF containing (in mM): 92 NMDG, 2.5 KCl, 1.25 NaH_2PO_4, 30 $NaHCO_3$, 20 HEPES, 25 glucose, 2 thiourea, 5 Na-ascorbate, pH adjusted to 7.3-7.4 with HCl. Brains were extracted and 320 mm-thick coronal slices were obtained. Slices were transferred to a pre-warmed (32 °C) chamber with NMDG-based ACSF and kept for 11 minutes. Slices were then transferred to a maintaining solution containing (in mM): 92 NaCl, 2.5 KCl, 1.25 NaH_2PO_4, 30 $NaHCO_3$, 20 HEPES, 25 glucose, 2 thiourea, 5 Na-ascorbate, 3 Na-pyruvate, 2 $CaCl_2$, 2 $MgSO_4$ for at least 1h before recording. For electrophysiological recordings, slices were transferred to a recording chamber perfused with ACSF containing (in mM): 124 NaCl, 2.5 KCl, 1.25 NaH_2PO_4, 24 $NaHCO_3$, 5 HEPES, 12.5 glucose, 2 $CaCl_2$, 2 $MgSO_4$. 3-5 MΩ resistance borosilicate glass pipettes were filled with a $KMeSO_3$-based internal solution containing (in mM): 135 $KMeSO_3$, 4 $MgCl_2$, 10 HEPES, 4 Na-ATP, 0.4 Na-GTP, 5 phosphocreatine, pH 7.2, 290 mOsm. Cells were recorded in current-clamp configuration. Current steps from -20 to 200 pA were applied in 5 pA steps for 100 ms, and the rheobase was determined as the minimum amount of current eliciting an action potential. After obtaining a baseline rheobase, 10 mM PSEM was perfused onto the slice for 5-10 min, and the rheobase was determined again.

Pharmacology in vivo

Local delivery of SCH23390 (1.5mM in saline per side, Sigma; D1/5 dopamine receptor antagonist) was used to prevent long-term memory consolidation at indicated brain areas bilaterally.

Ablation of dopamine neurons projecting to TS bilaterally was done as previously described (Menegas et al., 2018). Briefly, a solution of 28.5 mg desipramine (Sigma-Aldrich, D3900-1G), 6.2 mg pargyline (Sigma-Aldrich, P8013-500MG), 10 mL water, and NaOH to pH 7.4 was prepared and injected i.p. to animals at 10 mg/kg. This solution prevents dopamine uptake in noradrenaline neurons, and increases the selectivity of uptake by dopamine neurons. Next, a solution of 10 mg/mL 6-hydroxydopamine (6-OHDA; Sigma-Aldrich, H116-5MG) in 0.2% ascorbic acid (Sigma-Aldrich, PHR1008-2G) in saline (0.9% NaCl; Sigma-Aldrich, PHR1008-2G) was injected bilaterally during stereotactic surgeries as described above into TS. The saline solution included a small amount of ascorbic acid to prevent 6-OHDA from breaking down. To further protect 6-OHDA from breaking down, this solution was kept on ice, wrapped in aluminum foil, and used within 3 h of mixing. If the solution turned brown, it was discarded, as this indicates that the 6-OHDA had broken down.

Histological verification of injection sites

Mice were anesthetized with isoflurane (5% in O2) before injection of a Ketamine/Xylazine cocktail (90mg/kg and 10mg/kg), and were then transcardially perfused with ice-cold 4% paraformaldehyde in 0.1 M phosphate buffered saline. Brains were kept in fixation solution overnight at 4 °C before cutting 100um slices with a Vibratome. Viral expression spreads of rAAV9-CBA-flox-PSAM(Leu141-Phe,Tyr116Phe)GlyR-WPRE (inhibitor; Vector Biosystems Inc) was controlled by expression of its respective EGFP fluorophore. α-Bungarotoxin, Alexa 488 Conjugate (Molecular Probes, Life Technologies), was used 1:1000 to detect the expression of rAAV9-CAGflox-PSAM(L41FY116F)5HT3-WPRE (activator; Vector Biosystems Inc). Primary antibodies used in this study were rabbit anti-Tyrosine Hydroxylase at 1:1000 (EMD Millipore, AB152) and rabbit anti Parvalbumin (Swant, PV27) at 1:5000. Secondary antibody was donkey anti rabbit Alexa Fluor 657 (Invitrogen; A31573) at 1:1000.

In experiments involving injections with picospritzer, serial slices were imaged at 10× using Axio Scan.Z1 to locate the injection site and the extent of volume spread. Images for the analyses were taken at 40x using an Axio Imager M2 (upright microscope) equipped

with a Yokugawa CSU W1 Dual camera T2 spinning disk confocal scanning unit and VisiView software. Image stitching and analysis was performed using FIJI/ImageJ 1.53c software.

METHODS DETAILS

Male mice of closely comparable age were assigned randomly to experimental groups. The number of animals to be used for a standard behavioral analysis was determined based on preliminary behavioral experiments across different investigators in the laboratory. Data for each set of experiments has been acquired on a minimum of 3 independent days. For behavioral analysis, all data were collected with a video camera. The analysis of behavior was verified by a co-worker blind to experimental conditions.

We noticed increased injurious self-grooming in approx. 20% of stock animals from the age of 3 months and in almost 70% of all breeding animals after the second litter. Injured animals were excluded from all experiments. Additionally, occasional mice in which the viral injections had also targeted neighboring brain areas were excluded from the analysis.

QUANTIFICATION AND STATISTICAL ANALYSIS

Statistical analyses were performed in GraphPad PRISM 8 (GraphPad software Inc). Data distributions were tested by the Shapiro-Wilk normality test and based on significance a Gaussian distribution was assumed for all statistical calculations. Depending on dataset, unpaired Student's t- tests with Tukey's post-hoc analyses, one-way Anova followed by Tukey's or two-way-RM- ANOVA, followed by Sidak's post hoc test based on two-tailed comparisons were performed; $P < 0.05$ in post hoc comparisons. All results are presented as mean ± s.e.m. The sample size per group is mentioned in the respective figure legends ($n = 8$ for most experiments). Number of animals to be used for a standard behavioral analysis was determined based on our preliminary behavioral experiments across different investigators in the laboratory. Male mice of closely comparable age were assigned randomly to experimental groups. For behavioral analysis, all data were collected with a video camera. The analysis of behavior was verified by a co-worker blind to experimental conditions. Noldus Ethovision XT12 was used for automated analyses of movement and paths. Repetitive and exploratory behavior were quantified manually.